Swelling and mass transport properties of nanocellulose-HPMC composite films

Mikael Larsson[a,b,c], Anders Johnsson[a,b], Sofie Gårdebjer[a,d], Romain Bordes[a,b*] Anette Larsson[a,b]

[a]Department of Chemistry and Chemical Engineering, Chalmers University of Technology, 412 96 Goteborg, Sweden

[b]SuMo Biomaterials, a VINN Excellent Center at Chalmers University of Technology, 412 96 Goteborg, Sweden

[c]Future Industries Institute, University of South Australia, Mawson Lakes Campus, Mawson Lakes, SA 5095 Australia

[d]Department of Theoretical Chemistry, Lund University, 221 00 Lund, Sweden

*Corresponding author: bordes@chalmers.se

Abstract

Composite films were sprayed from mixtures of water soluble hydroxypropyl methylcellulose (HPMC) and either nanofibrillated cellulose (NFC) or cellulose nanocrystals (CNC). Fiber diameter was similar for both nanocelluloses but fiber length was several µm for NFC and about 200 nm for CNC. Films were characterized for morphology, swelling, mass loss and transport properties. NFC-HPMC films swelled less than CNC-HPMC films; with a HPMC content of 20wt% NFC-HPMC and CNC-HPMC films presented swelling of 7 and 75 g/g, respectively. The swelling strongly influenced water transport across the films, with slower transport for CNC-based materials compared to NFC-based materials. The properties of NFC-based films were comparable to previous results using microfibrillated cellulose (MFC) with heterogeneous structural content and fiber lengths of ~10 µm. The findings have implications for using nanocellulose to modulate material properties in wet-state applications, with effects being in strong contrast when using as a hardening filler in dry materials.

Keywords: Cellulose nanocrystals, composite films, controlled release, microfibrillated cellulose, nanofibrillated cellulose, structure.

Graphical abstract:

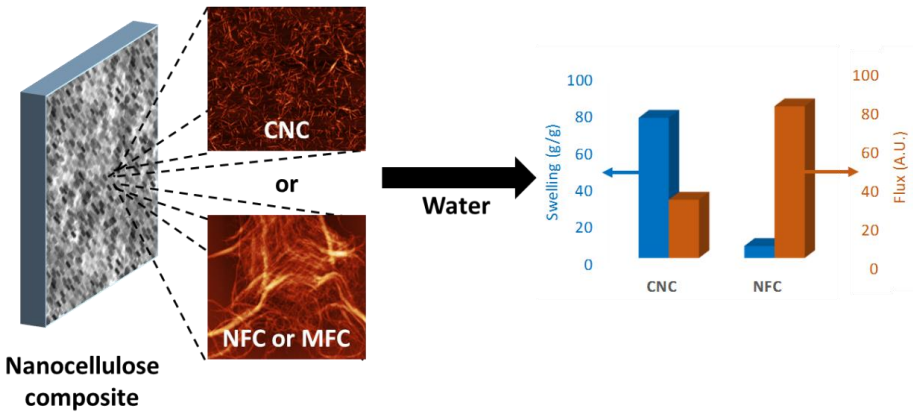

1. Introduction

In the search for renewable materials to replace fossil-based plastics, pure nano-dimensioned cellulose and composite films have received great interest as barrier materials in recent years [1-6]. The majority of investigations have focused on dry-state barriers and gas permeability. However, recently such systems have also received interest for use as a barrier against liquid [5-9]. Recent advances in chemistry and processing of nanocellulose have greatly facilitated such development [3, 10]. Three different types of cellulose, with varying lengths and diameters are commonly studied: nanofibrillated cellulose (NFC), microfibrillated cellulose (MFC) and cellulose nanocrystals (CNC). NFC is also sometimes referred to as microfibrillated cellulose, nanofibrils and/or microfibrils, and typically presents diameters of some nanometres to about 100 nm and lengths of several micrometers, while CNC typically presents similar ranges in diameters, but lengths of some hundreds of nanometers, or possibly longer if sourced from non-plant organisms [3]. The larger length compared to diameter results in large aspect ratios for both NFC and CNC, with that of NFC typically being more than an order of magnitude larger than that of CNC (Table 1).

Nanosized cellulose with large aspect ratios is finding use as a filler to improve mechanical properties in dry [11] and wet [12] materials. Along those lines NFC and CNC have started to receive interest for use in controlled release applications; NFC for modulating substance release by delayed diffusion through the nano-microporous network [7, 13, 14] and CNC as a carrier that physically adsorbs substances onto its surface [15, 16]. Previous work in our group revealed that MFC films produced via solvent casting formed swollen nano-microporous films in the wet-state and that the permeability and swelling could be controlled by adding the food- and pharmaceutically-approved water-soluble polymer hydroxypropyl methyl cellulose (HPMC) to prepare composite films [7]. In contrast to conventional controlled release films where HPMC can be used as a pore former to increase the permeability [17], the permeability decreased with increasing HPMC content in the MFC films. It was shown that the presence of HPMC modulated the film structure and swelling properties, and that a large portion of the HPMC remained in the films after submersion. It was also shown that the water permeability increased when 20% (w/w) HPMC was added to the films, but decreased when an amount larger than 35% (w/w) HPMC was added to the composite films.

Sample name	Length (nm)	Width (nm)	Aspect ratio[a]	Surface chemistry	Surface charges (Zeta potential)	Preparation method	Notes
MFC [b,c]	500-10 000's	1-1000's	>1-200	OH	N/A	From commercial bleached Kraft pulp: Mechanical pre-treatment followed by homogenization.	Highly heterogeneous; containing particles, fibers and fiber clusters, ranging from nanometers to hundreds of micrometers in size.
NFC[b]	500-2000	4-20	>100	OH	N/A	From softwood sulfite dissolving pulp: Enzymatic pre-treatment followed by homogenization	Predominantly nanofibres
CNC[b]	170 (50-500)	17 (3-5)	~10	OH and sulfate	-42 mV	From microcrystalline cellulose: Acid hydrolysis	Only nanocrystals observed

[a]From length and width estimates.

[b]Values estimated from the AFM and light scattering done in our group. Values in bracket reported from literature [18].

[c]Values from a previous characterization [19].

Table 1. Colloidal characteristics of used celluloses.

In this study, it was hypothesized that the swelling and water permeability of pure and composite films from three different nano-dimensioned celluloses (NFC, MFC and CNC) would depend on the aspect ratio of the used cellulose. The permeability, swelling and structure of spray-dried films of pure cellulose or composites containing HPMC were

analyzed and results were compared with solvent-casted MFC-HPMC films from our previous work [7]. The structure of the cellulose fibers was characterized with atomic force microscopy (AFM) and dynamic light scattering (DLS) for the CNC. Film structures were characterized with scanning electron microscopy (SEM) and the water permeability was determined using radiolabeled (tritated) water. Swelling behavior of the composite films was determined through gravimetric analysis. The results provide important information on the performance and robustness of nanocellulose films in the wet state with regard to structure and preparation conditions. The findings are highly relevant for the utilization of nano-dimensioned cellulose in materials for which controlled transport properties are of major importance, for example controlled release of pharmaceutical drugs or wound care products.

2. Materials and methods

Sodium hydroxide (anhydrous pellets, reagent grade ≥98%), dialysis membrane Dowex Marathon MR-3 hydrogen form, polyethyleneimine (50% (w/v), M_w 750 000), and sulfuric acid (ACS reagent, 95.0-98.0% (w/w)) were purchased form Sigma-Aldrich, Germany. ^{3}[H]-water and scintillation liquid Ultima Gold® were purchased from Perkin Elmer, USA and used as received. HPMC (Metolose 90SH100 SR), and microcrystalline cellulose (Avicel PH-101 NF) were gifts from Shin-Etsu Chemical Co., Ltd., Tokyo, Japan and FMC BioPolymer, USA, respectively. NFC generation 1 was kindly provided by Innventia AB, Sweden, and was produced from softwood sulfite dissolving pulp by enzymatic treatment with subsequent homogenization [20]. Water was purified with Millipore Milli-Q Purification system (resistivity > 18.2 MΩ cm).

2.1. Production of cellulose nanocrystals (CNC)

CNC were prepared by adapting the preparation method earlier reported [21, 22]. Briefly, 40 g of microcrystalline cellulose (Avicel PH-101 NF) was dispersed in 400 ml Milli-Q water in a 2 liter Erlenmeyer flask while stirred and cooled by an ice bath. Sulfuric acid was added drop-wise to reach a final concentration of 64% (w/w) while the temperature was kept below 20°C. The reaction was initiated by heating the mixture to 45°C, and left to react under vigorous stirring for 70 minutes. The reaction was quenched with a 10-fold addition of deionized water and was centrifuged at 5100 rpm (Sigma 4K15 centrifuge, UK) in 5 minutes cycles where the supernatant was discarded and replaced by deionized water. This was

repeated until the supernatant became turbid. The cellulose was put on dialysis against deionized water, which was changed two times daily until the conductivity did not differ from the pure deionized water. The dialyzed cellulose was then ion exchanged (Dowex Marathon MR-3 resin, hydrogen form) under continuous stirring for 48 h. The mixture was filtered through a fritt disc glass funnel (n°2) to separate the cellulose from the resin. The cellulose was finally sonicated (Vibracell Sonicator, Sonics and Materials Inc., Danbury, CT) at 40% output in three cycles of 14 minutes each, and subsequently titrated by conductometry with a NaOH solution (0.02 M). A final centrifugation step was carried out to remove large aggregates (5100 rpm, 5 minutes), resulting in suspension with a dry weight of ~0.5% (w/w). The suspension was concentrated up to 1% (w/w) by rotary evaporation.

2.1.2. Characterization of nanocelluloses

The NFC and CNC were imaged with a NTEGRA Prima from NT-MDT (Ireland) in tapping mode under ambient air conditions (23°C and 48% relative humidity). No image processing except flattening was made. AFM measurements were performed using a single crystal silicon tip with a radius of 10 nm (NT-MDT, NSG01). Samples were prepared as follow: a 20 µl 0.1% w/v polyethyleneimine drop was put on a mica sheet freshly cleaved for three minutes then rinsed with water and dried with nitrogen gas. Subsequently a 20µl drop 0.05% w/w CNC or NFC suspension was deposited on the mica surface for three minutes, then rinsed and dried with nitrogen gas.

2.2. Preparation and characterization of composite films

The NFC was diluted with Milli-Q water to a final concentration of 1% (w/w) and was dispersed for 1 minute at 24,000 rpm using a homogenizer (DI 18 basic, Ika). The CNC suspension was used at 1% (w/w). A 3% (w/w) stock solution of HPMC was prepared in Milli-Q water. Mixtures containing 0, 10, 20, 27 and 35% (w/w) HPMC and CNC or NFC were prepared by weighing. Finally, the total NFC-HPMC concentration was adjusted to 1 % (w/w) and the total CNC/HPMC to 0.5 % (w/w). Each mixture was sprayed with a spray gun onto a weighing boat placed on a rotating heated metal plate to ensure homogeneous spraying. To reduce the evaporation time the films were heated from above with hot air. Finally, the weighing boat was placed in an oven at 40-50°C for further drying overnight. The CNC-HPMC films obtained were transparent while the NFC-HPMC films were partly opaque.

2.2.1. Swelling tests and loss of mass

The swelling tests were performed on cut-out square film pieces with weights in the range of 5 to15 mg using a dissolution bath. The films were placed in USP-1 baskets that were submerged in 900 ml Milli-Q water at 37°C under stirring at 50 rpm. At specific times, the baskets with the films inside were taken out, carefully dried with paper tissues, and the weights were measured. The swelling ratio was calculated as:

$$SR = \frac{W_2 - W_1}{W_1} \qquad (1)$$

where *SR* is the swelling ratio, W_1 is the initial weight of film, and W_2 is the weight of swelled film derived as:

$$W_2 = B_F - B_0 \qquad (2)$$

where B_F is the weight of basket with swelled film, and B_0 is the average weight of the same cage without film but exposed to the same conditions (n ≥ 10 samples).

For the CNC-HPMC films the swelling was measured for 100 minutes (due to rapid loss of mass). For the NFC-HPMC films, the measurement was conducted for 180 minutes (same time as the mass transport tests).

After the swelling tests, the film pieces were placed in an oven and dried over night at 50°C. The weights of the dried film pieces were measured and the loss of mass index was calculated as:

$$LM\% = \frac{W_1 - W_3}{W_1} * 100\% \qquad (3)$$

where *LM* is the loss of mass, W_1 is the initial weight of the film and W_3 is the weight of the dried film.

2.2.2. Film morphology

The cross-sections were studied using a scanning electron microscope (Leo Ultra 55 FEG-SEM, LeoElectron Microscopy Ltd, UK) with a secondary electrons detector at 3 kV in vacuum. Prior to analysis, films swollen for 30 minutes were frozen in liquid nitrogen and freeze-dried. Samples of film as prepared and freeze-dried were coated with a thin gold layer to avoid charging of the samples.

2.2.3. Mass transport properties

Mass transport measurements were performed in diffusion cells at 37°C under stirring (200 rpm). Details on the setup can be found elsewhere [23]. Briefly, 15 ml of pre-heated Milli-Q water was added simultaneously to both compartments, followed by immediate addition of 10 µl ^{3}[H]-labelled water to the donor chamber. The permeation was monitored by taking out samples of 500 µl from the acceptor compartment at determined times, and immediately replacing them with equal amounts of pre-heated Milli-Q water. Samples were assayed with scintillation liquid, Ultima Gold®, and analyzed in a liquid scintillation counter (Tri-Carb B2810TR, Perkin-Elmer, USA). When a sample containing tritiated water is mixed with the scintillation liquid a signal expressed in DPM (disintegrations per minute) is obtained. The signal is proportional to the concentration of ^{3}[H]-labelled water.

The accumulated radioactivity, RA_n, in the acceptor compartment at time t was determined as:

$$RA_n(t) = RA_{sample,n}(t)\frac{V_{tot}}{V_{sample}} + RA_{n-1} \qquad (4)$$

where $RA_{sample\ n}$ is the radioactivity in sample n that is withdrawn at time t with a volume of V_{sample}, and V_{tot} is the total volume in the acceptor chamber.

The normalized radioactivity in the acceptor, NRA, at time t for sample n was calculated as:

$$NRA(t) = \frac{RA_n(t)}{RD(t=0)}\,100\% \qquad (5)$$

Where RD is the initial radioactivity in the donor compartment. The water mass transport was calculated by plotting NRA as function of the time. It is assumed during the course of the experiment that the amount of ^{3}[H]-labelled water transferred from the donor chamber to the acceptor chamber is negligible in comparison with the starting concentration in the donor chamber.

3. Results and discussion

3.1. Characterization of the nanocelluloses

Atomic force microscopy (AFM) was used to characterize the morphology of the NFC and CNC. MFC has been previously characterized [19]. From Fig. 1 it is evident that the length of NFC much exceeded that of CNC, while the diameter was similar. The CNC showed diameters between 10 to 20 nm and lengths of approximately 200 nm, yielding an aspect ratio

of about 10, in agreement with previous reports [18, 21, 24]. The NFC had a fiber diameters in the range 4-20 nm, lengths of up to 2 µm and aspect ratios >100. In contrast, the MFC was highly heterogeneous, containing both smaller fragments with low aspect ratio, extremely long and entangled nanofibers, and microfibers and bundles [19]. Thus, the three materials represented distinctively different nanocelluloses. CNC had a low aspect ratio compared to NFC and MFC. On the other hand, the structural content of MFC was highly heterogeneous compared to that of NFC and CNC. See Table 1 for summary of the structural properties of CNC, NFC and MFC.

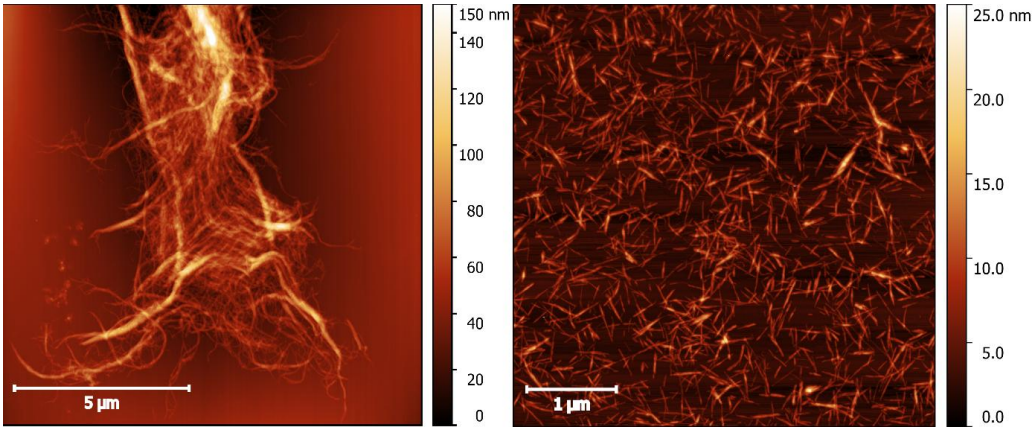

Figure 1. Atomic force microscopy (AFM) image recorded in tapping mode of NFC (left) and CNC (right) on a glass plate coated with polyethylenimine at 23°C and 48% relative humidity.

3.2. Characterization of the composite films

3.2.1. Swelling behavior

In previous work it was reported that the swelling of MFC-HPMC composite films increased with HPMC content and that a fraction of the of the HPMC was released from the films [7]. In this study, the swelling behavior of CNC-HPMC and NFC-HPMC films was investigated in Milli-Q water at 37°C for 100 and 180 minutes, respectively (Fig. 2a-b) and the results were compared with those previously reported for MFC-HPMC films (Fig. 3). Due to the fragile nature of CNC-HPMC composites, a modified method involving placement of the films in

baskets was used for submerging the films in the present work, see Materials and Methods. Even under these protective conditions the CNC-HPMC films with ≥ 20% HPMC rapidly lost mass and were fragmented, only maintaining coherency for about 100 minutes. CNC films containing less than 20% HPMC (w/w) remained coherent for the 180 minutes of the experiment (pure CNC films actually maintained structural integrity for more than one week). The swelling of NFC-HPMC films was possible to measure for 180 minutes.

The swelling of the NFC-HPMC films over time is presented in Fig. 2a. The films turned from opaque to white when exposed to the Milli-Q water. Regardless of HMPC content, the samples presented rapid initial swelling so that a plateau was reached already at the first time-point of 10 minutes. The largest swelling ratio of 11 g/g was obtained for the film with 35% (w/w) HPMC content. Generally, the swelling increased with increasing HPMC content, but the swelling's dependence on HPMC content may be non-trivial over time. A detailed analysis was not possible given the magnitude of the error bars.

The CNC-HPMC films presented a different trend in swelling with HPMC content (Fig. 2b) than the NFC-HPMC films. First, not all films reached a plateau within the 100 minutes of the experiment. It was noted that films with high HPMC content lost material over the experiment, as substantiated by the sample with 35% HPMC decreasing in weight between the last time points. Secondly, the CNC-HPMC films exhibited swelling ratios about ten times larger than the NFC-based films. Pure CNC films presented rapid initial swelling and reached a plateau at 6 g/g after 10 minutes, the value was slightly larger than for pure NFC films, but the behavior was qualitatively similar. The film containing 10% HPMC had larger swelling than the pure CNC film and did not reach plateau. At the same time the swelling ratio was lower for this film compared to CNC-based films containing more HPMC. The highest swelling ratio of around 75 g/g was obtained for the film containing 20% HPMC after 100 minutes, at which time the swelling was still increasing. The films containing 27% and 35% HPMC presented similar swelling behavior to the one with 20% HPMC up to 30 minutes. After this time the 20% HPMC film continued to swell, while the latter 27 and 35% HPMC films seems to reach a plateau at about 40 g/g. This was likely due to the swelling being counteracted by material being eroded from the films. To summarize, for CNC-HPMC films the swelling was larger and seemed to have a more complicated dependence on the HPMC content than for NFC-HPMC films.

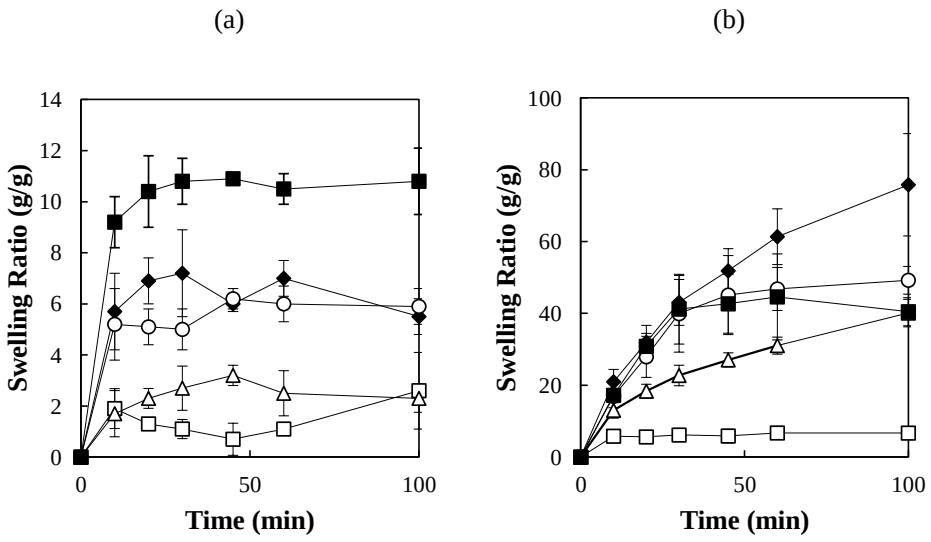

Figure 2. Swelling ratio versus time for (a) NFC and (b) CNC films with 0% (□), 10% (Δ), 20% (♦), 27% (○) and 35% (■) w/w HPMC. Error bars indicate standard deviation (n = 3).

In Fig. 3 comparison is made between the swelling ratios of CNC- (white), NFC- (grey) and MFC-based (black) films with varying HPMC content. The swelling ratios are reported up to 100 minutes ~~for the CNC-based films and at 180 minutes the NFC- and MFC-based films~~. It can be seen that the swelling ratio is highest for CNC-HPMC films for all amounts of added HPMC.

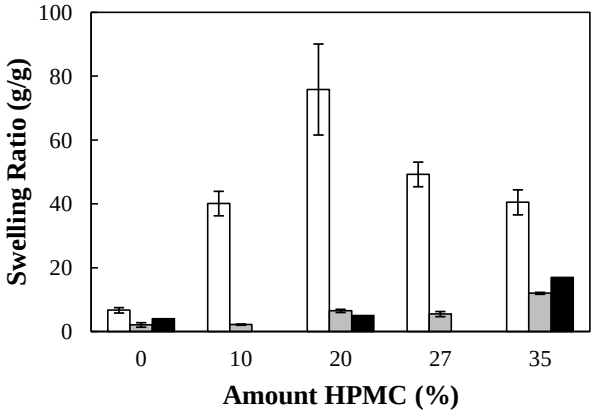

Figure 3. Swelling ratio for CNC-HPMC (white) after 100 minutes, NFC-HPMC (grey) and MFC-HPMC films (black) after 180 min. Error bars indicate standard deviation for CNC and NFC (n = 3). Data for MFC-HPMC are from [7].

For pure nanocellulose films the swelling ratio, measured as relative increase of mass, depends on the water ingress and displacement in the system. The water in swollen films of pure nanocellulose can be considered in two ways: (i) water is adsorbed to the surface of the nanocelluloses and to some extent penetrate into the nanocellulose fibers (leading to swelling of the nanofiber itself) and/or (ii) the pores are partly filled with water through capillary transport. The water transport can deform the film and lead to an increase of the macroscopic dimensions and a corresponding substantial decrease of the nanocellulose concentration. It is impossible to completely distinguish between these scenarios. However, if the main contribution to the swelling was water uptake of the fibers, a smaller swelling ratio would be expected for the crystalline CNC film compared to the two fibrous nanocelluloses. Since the opposite was observed (see Fig 3), it seems likely that the dominating mechanism for water uptake was capillary transport of water into the inter-cellulose space in the films.

The high swelling ratio of 75 g/g for 20% (w/w) CNC-HPMC composites and the swelling of the composite films in general can be rationalized by looking at the mechanism behind swelling of materials from water-soluble polymers. The first important step in this discussion is the mechanistic understanding of swelling of pure HPMC films, which coincides with the mechanism described in the literature for swelling of HPMC matrixes in controlled drug applications [25, 26]. When a dry HPMC material is exposed to water it will diffuse into the material, resulting in a water-concentration gradient. The water will plasticize the glassy

HPMC, causing a transition to the rubbery state, in which the swollen material is best described as a semi-dilute polymer solution [27]. The rate of the water ingress into the material is determined in-part by water´s chemical potential gradient. One major factor that drives water diffusion and facilitates the dilution of the system (here seen as swelling) is the gain in conformation entropy of the HPMC chains. The dilution lead to a decrease in the polymer concentrations and when the HPMC concentration is close to or below the overlap concentration, the polymer will be disentangled and released from the surface of the film [28].

An interesting observation is that the swelling ratio versus time reaches a plateau for several of the HPMC/nanocellulose films (see Figs. 2a-b). To give a plausible explanation for this one need to discuss the factors counteracting the swelling process. These films contain a highly percolated fiber network that will prevent welling when the energy gain from further water absorption is balanced by the energy cost to deform the film. The shear modulus is higher for a network of longer fibers compared to that of a corresponding network of shorter fibers [29]. As such the energy cost of deformation should increase with fiber length. Therefore, for the same amount of HPMC, i.e. the main driving force to swell the network, films of long fibers should present a lower equilibrium swelling than films of short fibers. This explains why films based on short CNC fibers swelled more than films based on longer NFC and MFC fibers for the same HPMC content (Fig 3).

The swelling ratio of a pure HPMC matrix tablet is known to be around 2, i.e. much less than what we observed for HPMC:nanocellulose films. A tentative explanation is that the highly percolated nature of the nanocellulose in the films provided a resistant armature that maintained film integrity and allow further swelling well beyond the point at which HPMC dissolve when used in a pure form.

In conclusion, we suggest that the driving force for swelling of HPMC-nanocellulose films is the presence of HPMC and that the counteracting force is the percolated network of nanocellulose, with longer NFC and MFC fibers restricting swelling more than shorter CNC fibers.

3.2.2. Loss of mass from films during swelling

The mass loss was determined at the final time point of the experiment and is presented in Fig. 4. The mass loss of NFC-based films appeared to have a linear dependence on HPMC

content. Compared to the films based on MFC the loss of mass was less for all HPMC contents. This could be explained by that the heterogeneous MFC contained significant amounts of small-sized particles and aggregates of low aspect ratios [7]. Those aggregates might not have been effectively entangled in the MFC network and could thus leave the films. Interestingly, for both NFC and MFC the mass loss was less than the mass content of highly soluble HPMC. For CNC-based films the mass loss was similar as for NFC at HPMC contents of 0 and 10% (w/w). However, above 10% (w/w) HPMC there was a dramatic increase in mass loss for the CNC-based films and the mass loss was larger than the mass corresponding to HPMC content, meaning that a fraction of the CNC was lost as well. This dramatic increase in mass loss above 10% (w/w) HPMC content is in agreement with the mechanism for release of materials from hydrophilic matrix systems [28]. As mentioned above, the release of HPMC from pure HPMC matrix occurs when the dilution of the polymer reaches the regime of the so-called overlap concentration, where individual chains begin to be released. In a refined model accounting for shear forces around the matrix, the overlap concentration is replaced by a critical polymer concentration at the outermost layer of the hydrophilic matrix. At the critical concentration the semi-dilute polymer solution cannot withstand the shearing forces caused by the stirring and therefore the polymer chains are released in the surrounding media. A similar mechanism can be applied to the HPMC-nanocellulose films. The nanocellulose network can withstand the shear forces above its percolation threshold. With an increased swelling the fiber concentration decreases and at high degrees of swelling the fibers can be eroded.

For the composite structures of HPMC and NFC or MFC, the ingress of water in the fiber network leads to dilution of the fiber network and HPMC. At low swelling ratios the strong armature nanocellulose fiber network can withstand the shear forces. However, hydrated HPMC will be diluted to concentrations around or below the overlap concentration and so that thus HPMC can disentangle and diffuse out from the films.

In the case of CNC-HPMC films the counteracting forces from the cellulose network on the swelling are low. For films with 10% (w/w) initial HPMC content a swelling ratio of 40 g/g and loss of mass of 7.4% was recorded after 100 minutes. The combined concentration of HPMC and CNC can be calculated to 2.2% (w/w) in this state (assuming a density equal to one). This is in the range of the percolation threshold of CNC [30, 31]. It is therefore likely that most of the HPMC had diffused out from the films but that the CNC network withstood the shear forces. Films with 20% (w/w) initial HPMC content presented a swelling ratio of 75

g/g and a mass loss of 60%. The combined concentration of HPMC and CNC can be calculated to 0.5% (w/w). This concentrations is below the percolation threshold of CNC and is in the range or below the overlap concentration of the HPMC used in this study [25]. Thus the mass loss was attributed both to dissolution of HPMC and erosion of the weak CNC network.

In conclusion, the loss of mass for both CNC- and NFC-HPMC composite films is suggested to be mainly due to dissolution of HPMC. However, for CNC-HPMC films with HPMC content above 10% the high swelling ratio and corresponding decrease in CNC concentration led to both HPMC and CNC being released from the films. This mechanism explain the swelling behavior of CNC-HPMC films and why the swelling of the 35 % (w/w) CNC-HPMC film seemingly passed through a maximum gravimetric swelling ratio over time. The same phenomenon is observed for hydrophilic matrix tablets [32, 33].

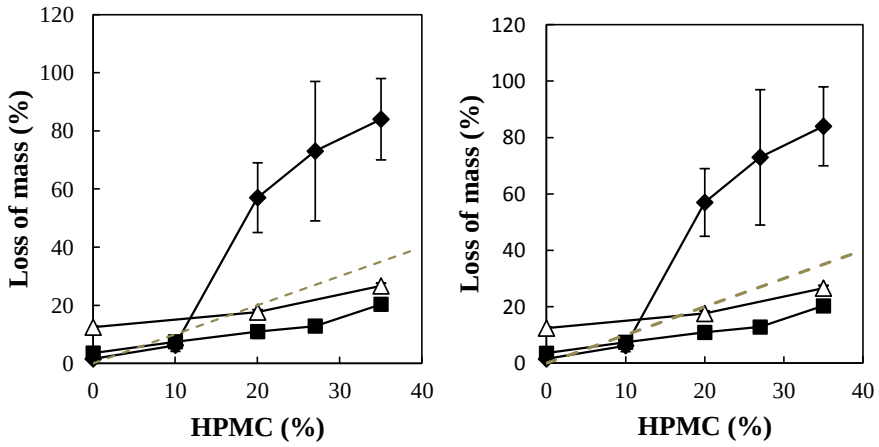

Figure 4. Loss of mass after swelling for CNC-HPMC (♦) (swollen for 100 min) and NFC-HPMC (■) and MFC-HPMC (△) (swollen for 180 min) films. Error bars indicate standard deviation (n = 3).The dashed grey line represent the maximal theoretical loss of HPMC.

3.2.3. Film morphology

The surface and cross-section morphology of the films prior to and after exposure to water was investigated with SEM. The surface of the films was homogeneous and did not show any

distinct features. Fig. 5 shows the cross section of the CNC (a and c) and NFC (b and d) films containing 20% (w/w) HPMC. Fig 5a-b are images of the cross-section of dry films cleaved before exposure to water and Fig. 5c-d are the cross-section of the corresponding films after exposure to water for 30 minutes, followed by quenching in liquid nitrogen, cleavage and freeze-drying.

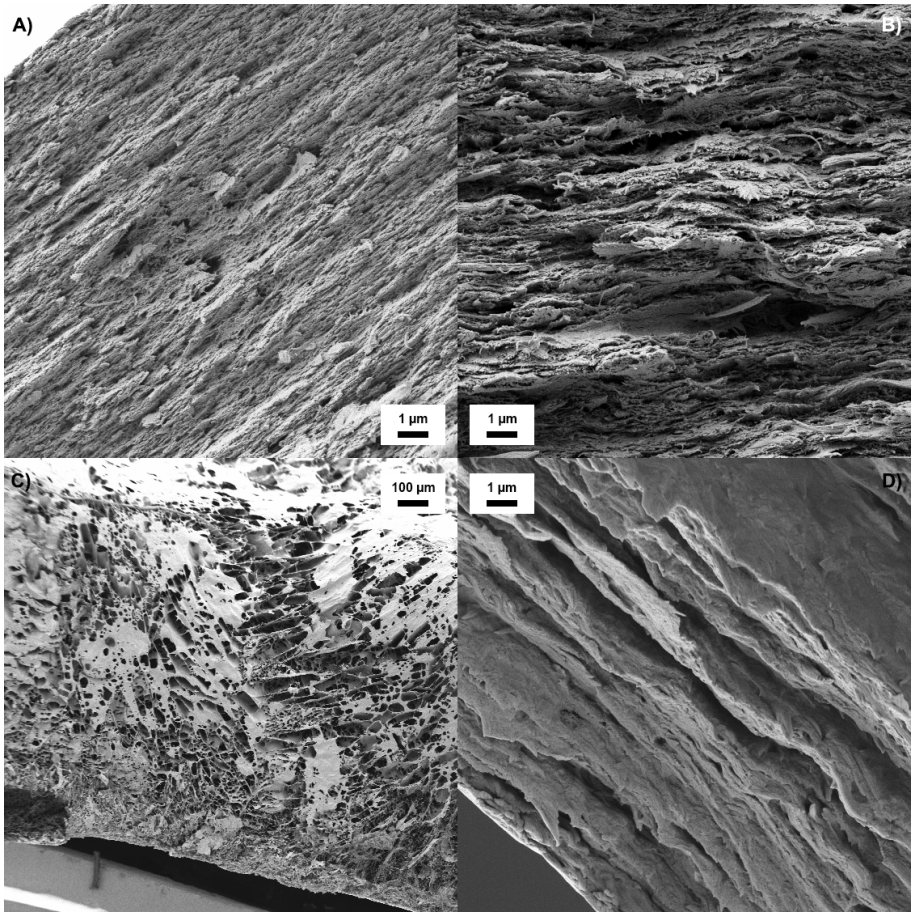

Figure 5. SEM Micrograph of a NFC and CNC films composed of 20% HPMC (w/w). (a) and (c) show the cross-section of CNC films after preparation before and after exposure to water, repesctively. Specimen (b) and (d) show the cross-section of the NFC films treated in the same way. The films exposed to water (c and d) were frozen in liquid nitrogen, cleaved and then freeze-dried. Note the 100 times larger scale bar in (c) compared to the other films.

The cross-section of the films after preparation showed that the CNC-based film was smother compared to the more fragmented/layered character of NFC based film, where each layer was estimated to be between 100 to 250 nm (Fig. 5). After exposure to water a highly swollen foam-like porous structure with large pores above 20 µm randomly oriented was observed for the CNC film, whereas the NFC films seemed to keep their layered structure aligned with the surface, in line with previous report for MFC [7]. Further interpretation on the pore-structure is rendered difficult as liquid nitrogen treatment is known to generate artifacts.

It seemed that the presence of HPMC did not significantly change the nanocellulose film forming properties, with CNC being more homogeneous while NFC formed a layered structure as previously observed [34, 35].

3.2.4. Mass transport properties

Having established differences in swelling behavior and film structure between CNC-based and NFC-based films and the similarity of the latter with MFC-based films, the wet-state barrier properties of the films were investigated. Tritiated water was used to monitor the water transport through the films at 37°C with stirring in both donor and acceptor compartments.

Pure films of CNC were too fragile to be placed in the diffusion cells, while pure NFC films as well as the composites could be analyzed. The corresponding data for the MFC-HPMC films was interpolated from previous work to simplify comparison [7]. The time dependency of the normalized radioactivity, *NRA*, of the tritiated water accumulated in the acceptor was plotted for CNC-, NFC- and MFC-HPMC films with various HPMC contents, as shown Fig. 6.

As expected from the similarities in swelling behavior and structure, the NFC-HPMC and MFC-HPMC presented similar mass transport properties. In addition, for both systems the transport across the films was decreased with increasing HPMC content. For the CNC-based films, the water transport through the films was slower than for NFC and MFC. As mentioned earlier, the CNC-films became very fragile and only the preparation with 10% (w/w) HPMC remained intact during the 180 minutes of the experiment. The transport of the tritiated water through the CNC-based films was similar irrespective of the HPMC content except for the higher fraction of HPMC (35% (w/w)) which showed lower mass transport rate. The trend in the transport through the nanocellulose films with different HPMC content can be more

clearly seen by looking at the fraction of tritiated water in the acceptor compartment at a fixed time of 60 minutes (Fig. 7).

(a) (b) (c)

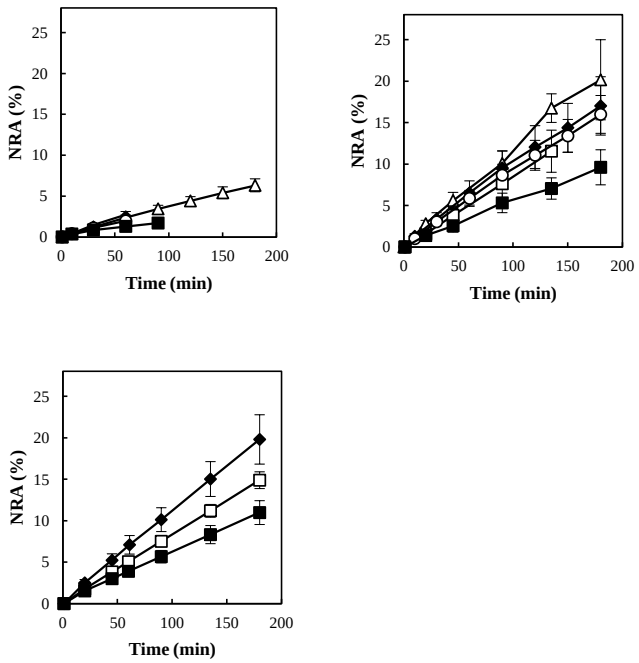

Figure 6. Normalized radioactivity in the acceptor after transport of tritiated water through films containing 0% (□), 10% (△), 20% (◆), 27% (○) and 35% (■) (w/w) HPMC. Error bars indicate standard deviation (n = 3). (a) CNC-HPMC; (b) NFC-HPMC; and (c) MFC-HPMC (n = 2 or 3). The same y-scale was used for all plots for a better comparison of the systems.

The mass transport rate across films depends on several of factors such as the level of hindrance the penetrant meets during the transport, typically fibers or polymer chains, the pathway for transport or the porosity of the system, for example. The CNC films will be more diluted (due to larger swelling and larger loss of mass) and thus have higher porosity than the NFC films. These properties should give larger mass transport for the CNC films compared to the NFC films. At the same time, an increased swelling of the films usually reduces the mass transport rate across the films due to an increased diffusion path. Fig. 7 shows that transport across CNC films was lower for all HPMC contents compared to the NFC and MFC films.

This means that the reduction in mass transport due to the large swelling is dominating over the pore formation and dilution of the nanocellulose films.

In summary, pure NFC films and HPMC containing composites presented wet-state barrier properties almost identical to those of MFC-based films, despite differences in structural content of the two nanofibril celluloses and between film preparation methods. The results indicate that the barrier properties are robust with regard to film preparation and structural content of the used nanofibril cellulose. In contrast, the CNC-based films did display a lower permeability, but the films were highly unstable and their use as a wet-state barrier seems limited. Potential solutions to this problem could be to increase the stability of the films by incorporating a swellable polymer that forms a crosslinked network *in situ*.

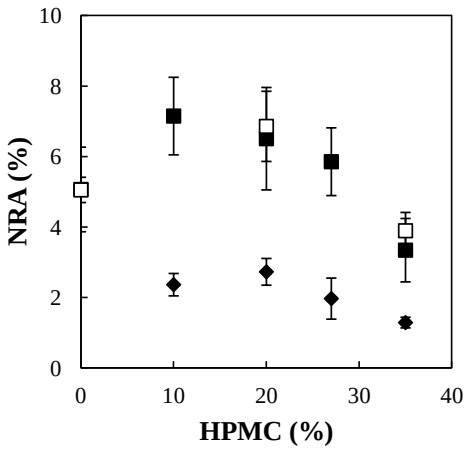

Figure 7. Normalized radioactivity in the acceptor after transport of water through films composed of CNC-HPMC (◆) NFC-HPMC (■) and MFC-HPMC (□) films after 60 minutes.

Conclusion

In this study, we investigated film properties for mixtures of the pharmaceutical approved cellulosic derivative HPMC with three different types of nanocelluloses. The length of the nanocelluloses in the HPMC:nanocellulose composite films appeared essential as it: (i) determined the structure of the formed composites: (ii) greatly impacted the films properties (swelling, mass transport, mass loss and integrity). Furthermore, a mechanistic model

explaining the observed dependence on the fiber length was suggested. Briefly, long fibers in the network generate larger resistance to deformation than short fibers, resulting in larger swelling for networks of short fibers (like CNC). The main driving force for swelling in these composites was the presence of the hydrophilic polymer (HPMC), which swelled and partly dissolved in water. The fiber network acted as an armature, which allowed a very large swelling of 75 g/g for the 20% (w/w) CNC-HPMC film after 100 minutes. At the same time, the mass loss of this film was as high as 60%, resulting in mechanical instability. For practical applications stable films are required and it is therefore important to tune the swelling by carefully choosing the length of used nanocellulose. For example, films from longer NFC fibers, also with 20% (w/w) HPMC, presented more restricted swelling (7 g/g) and were stable in water for more than a week. The increased diffusion length across the films due to swelling was the dominating factor in determining the water transport across the nanocellulose composite films. Even though the CNC-HPMC films were less dense and had larger mass loss, the water transport across them was slower than across corresponding NFC-HPMC films. Finally, all film properties were similar for films based on MFC or NFC, even though the films were prepared using very different methods. The NFC-HPMC films were sprayed using a spray gun, followed by drying at 50°C for several hours. MFC-HPMC films were produced by solvent casting for three weeks at under controlled conditions at 30°C. This indicates that the choice of manufacturing method for the films has much less influence on the film properties than the aspect ratio of the nanocellulose. The findings are highly relevant for further developments towards use of nanocellulose in wet-state applications

Acknowledgment

This project is part of the VINNOVA VINN Excellence Centre SuMo Biomaterials (Supermolecular Biomaterials—Structure dynamics and properties). The financial support from the Centre is gratefully acknowledged. Innventia AB is acknowledged for the kind gift of NFC.

References

Comment [RB1]: I could not really see the point of reviewer 2… some of the tile contained capital letter, which I have corrected. Still I could not spot any initial problem…he may have meant capital lette instead of initial…

[1] V. Kumar, R. Bollström, A. Yang, Q. Chen, G. Chen, P. Salminen, D. Bousfield, M. Toivakka, Comparison of nano- and microfibrillated cellulose films, Cellulose 21(5) (2014) 3443-3456.

[2] K. Syverud, P. Stenius, Strength and barrier properties of MFC films, Cellulose 16(1) (2009) 75-85.
[3] D. Klemm, F. Kramer, S. Moritz, T. Lindström, M. Ankerfors, D. Gray, A. Dorris, Nanocelluloses: A New Family of Nature-Based Materials, Angew. Chem. Int. Ed. 50(24) (2011) 5438-5466.
[4] N. Lavoine, I. Desloges, A. Dufresne, J. Bras, Microfibrillated cellulose – Its barrier properties and applications in cellulosic materials: A review, Carbohydr. Polym. 90(2) (2012) 735-764.
[5] S. Gardebjer, M. Andersson, J. Engstrom, P. Restorp, M. Persson, A. Larsson, Using Hansen solubility parameters to predict the dispersion of nano-particles in polymeric films, Polymer Chemistry 7(9) (2016) 1756-1764.
[6] S. Gårdebjer, A. Bergstrand, A. Larsson, A mechanistic approach to explain the relation between increased dispersion of surface modified cellulose nanocrystals and final porosity in biodegradable films, European Polymer Journal 57 (2014) 160-168.
[7] M. Larsson, J. Hjärtstam, A. Larsson, Novel nanostructured microfibrillated cellulose–hydroxypropyl methylcellulose films with large one-dimensional swelling and tunable permeability, Carbohydr. Polym. 88(2) (2012) 763-771.
[8] A.M. Slavutsky, M.A. Bertuzzi, Water barrier properties of starch films reinforced with cellulose nanocrystals obtained from sugarcane bagasse, Carbohydrate Polymers 110 (2014) 53-61.
[9] G. Rodionova, M. Lenes, Ø. Eriksen, Ø. Gregersen, Surface chemical modification of microfibrillated cellulose: improvement of barrier properties for packaging applications, Cellulose 18(1) (2011) 127-134.
[10] H.P.S. Abdul Khalil, Y. Davoudpour, M. NazrulIslam, A. Mustapha, K. Sudesh, R. Dungani, M. Jawaid, Production and modification of nanofibrillated cellulose using various mechanical processes: A review, Carbohydrate Polymers 99 (2014) 649-665.
[11] M. Samir, F. Alloin, A. Dufresne, Review of Recent Research into Cellulosic Whiskers, Their Properties and Their Application in Nanocomposite Field, Biomacromolecules 6 (2005) 612-626.
[12] M. Larsson, Q. Zhou, A. Larsson, Different types of microfibrillated cellulose as filler materials in polysodium acrylate superabsorbents, Chinese Journal of Polymer Science 29 (2011) 407-413.
[13] N. Lavoine, I. Desloges, C. Sillard, J. Bras, Controlled release and long-term antibacterial activity of chlorhexidine digluconate through the nanoporous network of microfibrillated cellulose, Cellulose (2014) 1-14.
[14] N. Lavoine, I. Desloges, J. Bras, Microfibrillated cellulose coatings as new release systems for active packaging, Carbohydrate Polymers 103 (2014) 528-537.
[15] R. Maren, D. Shuping, H. Anjali, L. Yong Woo, Cellulose Nanocrystals for Drug Delivery, in: K.J. Edgar, T. Heinze, C.M. Buchanan (Eds.), Polysaccharide Materials: Performance by Design, American Chemical Society, e-book, 2009, pp. 81-91.
[16] J.K. Jackson, K. Letchford, B.Z. Wasserman, L. Ye, W.Y. Hamad, H.M. Burt, The use of nanocrystalline cellulose for the binding and controlled release of drugs, International Journal of Nanomedicine 6 (2011) 321-330.
[17] P. Sakellariou, R.C. Rowe, E.F.T. White, Polymer/polymer interaction in blends of ethyl cellulose with both cellulose derivatives and polyethylene glycol 6000, International Journal of Pharmaceutics 34(1–2) (1986) 93-103.
[18] R.J. Moon, A. Martini, J. Nairn, J. Simonsen, J. Youngblood, Cellulose nanomaterials review: structure, properties and nanocomposites, Chem. Soc. Rev. 40(7) (2011) 3941-3994.

[19] M. Larsson, M. Stading, A. Larsson, High Performance Polysodium Acrylate Superabsorbents Utilizing Microfibrillated Cellulose to Augment Gel Properties, Soft Materials 8(3) (2010) 207-225.
[20] M. Pääkkö, M. Ankerfors, H. Kosonen, A. Nykänen, S. Ahola, M. Österberg, J. Ruokolainen, J. Laine, P.T. Larsson, O. Ikkala, T. Lindström, Enzymatic Hydrolysis Combined with Mechanical Shearing and High-Pressure Homogenization for Nanoscale Cellulose Fibrils and Strong Gels, Biomacromolecules 8(6) (2007) 1934-1941.
[21] D. Bondeson, A. Mathew, K. Oksman, Optimization of the isolation of nanocrystals from microcrystalline cellulose by acid hydrolysis, Cellulose 13 (2006) 171-180.
[22] M. Hasani, E.D. Cranston, G. Westman, D.G. Gray, Cationic surface functionalization of cellulose nanocrystals, Soft Matter 4(11) (2008) 2238-2244.
[23] J. Hjärtstam, T. Hjertberg, Studies of the water permeability and mechanical properties of a film made of an Ethyl Cellulose–Ethanol–Water ternary mixture, Journal of Applied Polymer Science 74(8) (1999) 2056-2056.
[24] L. Pranger, R. Tannenbaum, Biobased nanocomposites prepared by in situ polymerization of furfuryl alcohol with cellulose whiskers or montmorillonite Clay, Macromolecules 41(22) (2008) 8682-8687.
[25] A. Viridén, B. Wittgren, A. Larsson, Investigation of critical polymer properties for polymer release and swelling of HPMC matrix tablets, European Journal of Pharmaceutical Sciences 36(2–3) (2009) 297-309.
[26] A.R. Rajabi-Siahboomi, R.W. Bowtell, P. Mansfield, A. Henderson, M.C. Davies, C.D. Melia, Structure and behaviour in hydrophilic matrix sustained release dosage forms: 2. NMR-imaging studies of dimensional changes in the gel layer and core of HPMC tablets undergoing hydration, J. Controlled Release 31(2) (1994) 121-128.
[27] A. Körner, L. Piculell, F. Iselau, B. Wittgren, A. Larsson, Influence of different polymer types on the overall release mechanism in hydrophilic matrix tablets, Molecules 14(8) (2009) 2699.
[28] A. Körner, A. Larsson, L. Piculell, B. Wittgren, Molecular information on the dissolution of polydisperse polymers: mixtures of long and short poly(ethylene oxide), The Journal of Physical Chemistry B 109(23) (2005) 11530-11537.
[29] C.P. Broedersz, M. Sheinman, F.C. MacKintosh, Filament-length-controlled elasticity in 3D fiber networks, Physical Review Letters 108(7) (2012) 078102.
[30] V. Favier, H. Chanzy, J.Y. Cavaille, Polymer Nanocomposites Reinforced by Cellulose Whiskers, Macromolecules 28(18) (1995) 6365-6367.
[31] F. Du, R.C. Scogna, W. Zhou, S. Brand, J.E. Fischer, K.I. Winey, Nanotube networks in polymer nanocomposites: rheology and electrical conductivity, Macromolecules 37(24) (2004) 9048-9055.
[32] S. Abrahmsén-Alami, A. Körner, I. Nilsson, A. Larsson, New release cell for NMR microimaging of tablets: Swelling and erosion of poly(ethylene oxide), Int. J. Pharm. 342(1–2) (2007) 105-114.
[33] A. Körner, A. Larsson, Å. Andersson, L. Piculell, Swelling and polymer erosion for poly(ethylene oxide) tablets of different molecular weights polydispersities, J. Pharm. Sci. 99(3) (2010) 1225-1238.
[34] M. Henriksson, L.A. Berglund, P. Isaksson, T. Lindström, T. Nishino, Cellulose Nanopaper Structures of High Toughness, Biomacromolecules 9(6) (2008) 1579-1585.
[35] J. Huang, H. Zhu, Y. Chen, C. Preston, K. Rohrbach, J. Cumings, L. Hu, Highly Transparent and Flexible Nanopaper Transistors, ACS Nano 7(3) (2013) 2106-2113.

Swelling and mass transport properties of nanocellulose-HPMC composite films

Mikael Larsson[a,b,c], Anders Johnsson[a,b], Sofie Gårdebjer[a,d], Romain Bordes[a,b*] Anette Larsson[a,b]

[a]Department of Chemistry and Chemical Engineering, Chalmers University of Technology, 412 96 Goteborg, Sweden

[b]SuMo Biomaterials, a VINN Excellent Center at Chalmers University of Technology, 412 96 Goteborg, Sweden

[c]Future Industries Institute, University of South Australia, Mawson Lakes Campus, Mawson Lakes, SA 5095 Australia

[d]Department of Theoretical Chemistry, Lund University, 221 00 Lund, Sweden

*Corresponding author: bordes@chalmers.se

Abstract

Composite films were sprayed from mixtures of water soluble hydroxypropyl methylcellulose (HPMC) and either nanofibrillated cellulose (NFC) or cellulose nanocrystals (CNC). Fiber diameter was similar for both nanocelluloses but fiber length was several µm for NFC and about 200 nm for CNC. Films were characterized for morphology, swelling, mass loss and transport properties. NFC-HPMC films swelled less than CNC-HPMC films; with a HPMC content of 20wt% NFC-HPMC and CNC-HPMC films presented swelling of 7 and 75 g/g, respectively. The swelling strongly influenced water transport across the films, with slower transport for CNC-based materials compared to NFC-based materials. The properties of NFC-based films were comparable to previous results using microfibrillated cellulose (MFC) with heterogeneous structural content and fiber lengths of ~10 µm. The findings have implications for using nanocellulose to modulate material properties in wet-state applications, with effects being in strong contrast when using as a hardening filler in dry materials.

Keywords: Cellulose nanocrystals, composite films, controlled release, microfibrillated cellulose, nanofibrillated cellulose, structure.

Graphical abstract:

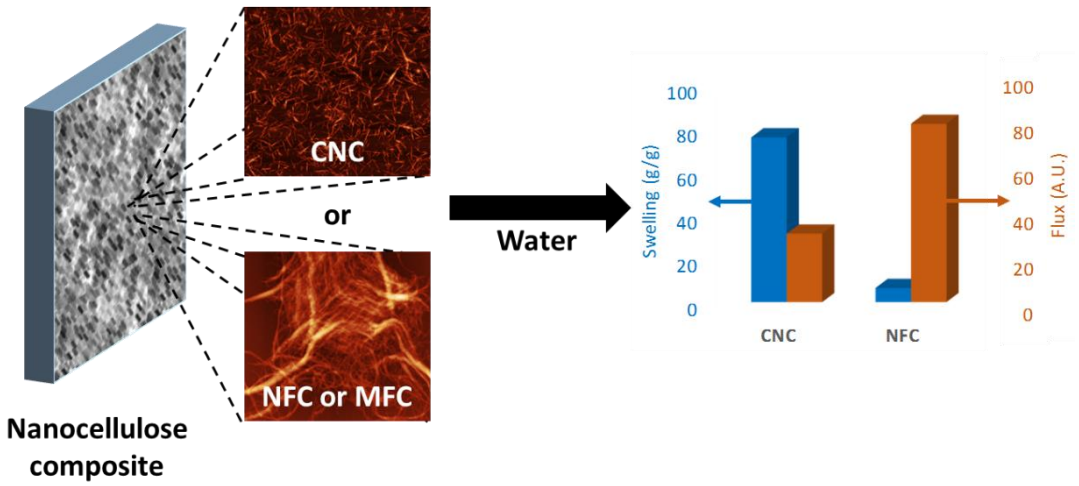

1. Introduction

In the search for renewable materials to replace fossil-based plastics, pure nano-dimensioned cellulose and composite films have received great interest as barrier materials in recent years [1-6]. The majority of investigations have focused on dry-state barriers and gas permeability. However, recently such systems have also received interest for use as a barrier against liquid [5-9]. Recent advances in chemistry and processing of nanocellulose have greatly facilitated such development [3, 10]. Three different types of cellulose, with varying lengths and diameters are commonly studied: nanofibrillated cellulose (NFC), microfibrillated cellulose (MFC) and cellulose nanocrystals (CNC). NFC is also sometimes referred to as microfibrillated cellulose, nanofibrils and/or microfibrils, and typically presents diameters of some nanometres to about 100 nm and lengths of several micrometers, while CNC typically presents similar ranges in diameters, but lengths of some hundreds of nanometers, or possibly longer if sourced from non-plant organisms [3]. The larger length compared to diameter results in large aspect ratios for both NFC and CNC, with that of NFC typically being more than an order of magnitude larger than that of CNC (Table 1).

Nanosized cellulose with large aspect ratios is finding use as a filler to improve mechanical properties in dry [11] and wet [12] materials. Along those lines NFC and CNC have started to receive interest for use in controlled release applications; NFC for modulating substance release by delayed diffusion through the nano-microporous network [7, 13, 14] and CNC as a carrier that physically adsorbs substances onto its surface [15, 16]. Previous work in our group revealed that MFC films produced via solvent casting formed swollen nano-microporous films in the wet-state and that the permeability and swelling could be controlled by adding the food- and pharmaceutically-approved water-soluble polymer hydroxypropyl methyl cellulose (HPMC) to prepare composite films [7]. In contrast to conventional controlled release films where HPMC can be used as a pore former to increase the permeability [17], the permeability decreased with increasing HPMC content in the MFC films. It was shown that the presence of HPMC modulated the film structure and swelling properties, and that a large portion of the HPMC remained in the films after submersion. It was also shown that the water permeability increased when 20% (w/w) HPMC was added to the films, but decreased when an amount larger than 35% (w/w) HPMC was added to the composite films.

Sample name	Length (nm)	Width (nm)	Aspect ratio[a]	Surface chemistry	Surface charges (Zeta potential)	Preparation method	Notes
MFC [b,c]	500-10 000's	1-1000's	>1-200	OH	N/A	From commercial bleached Kraft pulp: Mechanical pre-treatment followed by homogenization.	Highly heterogeneous; containing particles, fibers and fiber clusters, ranging from nanometers to hundreds of micrometers in size.
NFC[b]	500-2000	4-20	>100	OH	N/A	From softwood sulfite dissolving pulp: Enzymatic pre-treatment followed by homogenization	Predominantly nanofibres
CNC[b]	170 (50-500)	17 (3-5)	~10	OH and sulfate	-42 mV	From microcrystalline cellulose: Acid hydrolysis	Only nanocrystals observed

[a]From length and width estimates.

[b]Values estimated from the AFM and light scattering done in our group. Values in bracket reported from literature [18].

[c]Values from a previous characterization [19].

Table 1. Colloidal characteristics of used celluloses.

In this study, it was hypothesized that the swelling and water permeability of pure and composite films from three different nano-dimensioned celluloses (NFC, MFC and CNC) would depend on the aspect ratio of the used cellulose. The permeability, swelling and structure of spray-dried films of pure cellulose or composites containing HPMC were

analyzed and results were compared with solvent-casted MFC-HPMC films from our previous work [7]. The structure of the cellulose fibers was characterized with atomic force microscopy (AFM) and dynamic light scattering (DLS) for the CNC. Film structures were characterized with scanning electron microscopy (SEM) and the water permeability was determined using radiolabeled (tritated) water. Swelling behavior of the composite films was determined through gravimetric analysis. The results provide important information on the performance and robustness of nanocellulose films in the wet state with regard to structure and preparation conditions. The findings are highly relevant for the utilization of nano-dimensioned cellulose in materials for which controlled transport properties are of major importance, for example controlled release of pharmaceutical drugs or wound care products.

2. Materials and methods

Sodium hydroxide (anhydrous pellets, reagent grade ≥98%), dialysis membrane Dowex Marathon MR-3 hydrogen form, polyethyleneimine (50% (w/v), M_w 750 000), and sulfuric acid (ACS reagent, 95.0-98.0% (w/w)) were purchased form Sigma-Aldrich, Germany. ^{3}[H]-water and scintillation liquid Ultima Gold® were purchased from Perkin Elmer, USA and used as received. HPMC (Metolose 90SH100 SR), and microcrystalline cellulose (Avicel PH-101 NF) were gifts from Shin-Etsu Chemical Co., Ltd., Tokyo, Japan and FMC BioPolymer, USA, respectively. NFC generation 1 was kindly provided by Innventia AB, Sweden, and was produced from softwood sulfite dissolving pulp by enzymatic treatment with subsequent homogenization [20]. Water was purified with Millipore Milli-Q Purification system (resistivity > 18.2 MΩ cm).

2.1. Production of cellulose nanocrystals (CNC)

CNC were prepared by adapting the preparation method earlier reported [21, 22]. Briefly, 40 g of microcrystalline cellulose (Avicel PH-101 NF) was dispersed in 400 ml Milli-Q water in a 2 liter Erlenmeyer flask while stirred and cooled by an ice bath. Sulfuric acid was added drop-wise to reach a final concentration of 64% (w/w) while the temperature was kept below 20°C. The reaction was initiated by heating the mixture to 45°C, and left to react under vigorous stirring for 70 minutes. The reaction was quenched with a 10-fold addition of deionized water and was centrifuged at 5100 rpm (Sigma 4K15 centrifuge, UK) in 5 minutes cycles where the supernatant was discarded and replaced by deionized water. This was

repeated until the supernatant became turbid. The cellulose was put on dialysis against deionized water, which was changed two times daily until the conductivity did not differ from the pure deionized water. The dialyzed cellulose was then ion exchanged (Dowex Marathon MR-3 resin, hydrogen form) under continuous stirring for 48 h. The mixture was filtered through a fritt disc glass funnel (n°2) to separate the cellulose from the resin. The cellulose was finally sonicated (Vibracell Sonicator, Sonics and Materials Inc., Danbury, CT) at 40% output in three cycles of 14 minutes each, and subsequently titrated by conductometry with a NaOH solution (0.02 M). A final centrifugation step was carried out to remove large aggregates (5100 rpm, 5 minutes), resulting in suspension with a dry weight of ~0.5% (w/w). The suspension was concentrated up to 1% (w/w) by rotary evaporation.

2.1.2. Characterization of nanocelluloses

The NFC and CNC were imaged with a NTEGRA Prima from NT-MDT (Ireland) in tapping mode under ambient air conditions (23°C and 48% relative humidity). No image processing except flattening was made. AFM measurements were performed using a single crystal silicon tip with a radius of 10 nm (NT-MDT, NSG01). Samples were prepared as follow: a 20 µl 0.1% w/v polyethyleneimine drop was put on a mica sheet freshly cleaved for three minutes then rinsed with water and dried with nitrogen gas. Subsequently a 20µl drop 0.05% w/w CNC or NFC suspension was deposited on the mica surface for three minutes, then rinsed and dried with nitrogen gas.

2.2. Preparation and characterization of composite films

The NFC was diluted with Milli-Q water to a final concentration of 1% (w/w) and was dispersed for 1 minute at 24,000 rpm using a homogenizer (DI 18 basic, Ika). The CNC suspension was used at 1% (w/w). A 3% (w/w) stock solution of HPMC was prepared in Milli-Q water. Mixtures containing 0, 10, 20, 27 and 35% (w/w) HPMC and CNC or NFC were prepared by weighing. Finally, the total NFC-HPMC concentration was adjusted to 1 % (w/w) and the total CNC/HPMC to 0.5 % (w/w). Each mixture was sprayed with a spray gun onto a weighing boat placed on a rotating heated metal plate to ensure homogeneous spraying. To reduce the evaporation time the films were heated from above with hot air. Finally, the weighing boat was placed in an oven at 40-50°C for further drying overnight. The CNC-HPMC films obtained were transparent while the NFC-HPMC films were partly opaque.

2.2.1. Swelling tests and loss of mass

The swelling tests were performed on cut-out square film pieces with weights in the range of 5 to15 mg using a dissolution bath. The films were placed in USP-1 baskets that were submerged in 900 ml Milli-Q water at 37°C under stirring at 50 rpm. At specific times, the baskets with the films inside were taken out, carefully dried with paper tissues, and the weights were measured. The swelling ratio was calculated as:

$$SR = \frac{W_2 - W_1}{W_1} \qquad (1)$$

where *SR* is the swelling ratio, W_1 is the initial weight of film, and W_2 is the weight of swelled film derived as:

$$W_2 = B_F - B_0 \qquad (2)$$

where B_F is the weight of basket with swelled film, and B_0 is the average weight of the same cage without film but exposed to the same conditions (n ≥ 10 samples).

For the CNC-HPMC films the swelling was measured for 100 minutes (due to rapid loss of mass). For the NFC-HPMC films, the measurement was conducted for 180 minutes (same time as the mass transport tests).

After the swelling tests, the film pieces were placed in an oven and dried over night at 50°C. The weights of the dried film pieces were measured and the loss of mass index was calculated as:

$$LM\% = \frac{W_1 - W_3}{W_1} * 100\% \qquad (3)$$

where *LM* is the loss of mass, W_1 is the initial weight of the film and W_3 is the weight of the dried film.

2.2.2. Film morphology

The cross-sections were studied using a scanning electron microscope (Leo Ultra 55 FEG-SEM, LeoElectron Microscopy Ltd, UK) with a secondary electrons detector at 3 kV in vacuum. Prior to analysis, films swollen for 30 minutes were frozen in liquid nitrogen and freeze-dried. Samples of film as prepared and freeze-dried were coated with a thin gold layer to avoid charging of the samples.

2.2.3. Mass transport properties

Mass transport measurements were performed in diffusion cells at 37°C under stirring (200 rpm). Details on the setup can be found elsewhere [23]. Briefly, 15 ml of pre-heated Milli-Q water was added simultaneously to both compartments, followed by immediate addition of 10 µl ^{3}[H]-labelled water to the donor chamber. The permeation was monitored by taking out samples of 500 µl from the acceptor compartment at determined times, and immediately replacing them with equal amounts of pre-heated Milli-Q water. Samples were assayed with scintillation liquid, Ultima Gold®, and analyzed in a liquid scintillation counter (Tri-Carb B2810TR, Perkin-Elmer, USA). When a sample containing tritiated water is mixed with the scintillation liquid a signal expressed in DPM (disintegrations per minute) is obtained. The signal is proportional to the concentration of ^{3}[H]-labelled water.

The accumulated radioactivity, RA_n, in the acceptor compartment at time t was determined as:

$$RA_n(t) = RA_{sample,n}(t)\frac{V_{tot}}{V_{sample}} + RA_{n-1} \qquad (4)$$

where $RA_{sample\ n}$ is the radioactivity in sample n that is withdrawn at time t with a volume of V_{sample}, and V_{tot} is the total volume in the acceptor chamber.

The normalized radioactivity in the acceptor, NRA, at time t for sample n was calculated as:

$$NRA(t) = \frac{RA_n(t)}{RD(t=0)}\,100\% \qquad (5)$$

Where RD is the initial radioactivity in the donor compartment. The water mass transport was calculated by plotting NRA as function of the time. It is assumed during the course of the experiment that the amount of ^{3}[H]-labelled water transferred from the donor chamber to the acceptor chamber is negligible in comparison with the starting concentration in the donor chamber.

3. Results and discussion

3.1. Characterization of the nanocelluloses

Atomic force microscopy (AFM) was used to characterize the morphology of the NFC and CNC. MFC has been previously characterized [19]. From Fig. 1 it is evident that the length of NFC much exceeded that of CNC, while the diameter was similar. The CNC showed diameters between 10 to 20 nm and lengths of approximately 200 nm, yielding an aspect ratio

of about 10, in agreement with previous reports [18, 21, 24]. The NFC had a fiber diameters in the range 4-20 nm, lengths of up to 2 µm and aspect ratios >100. In contrast, the MFC was highly heterogeneous, containing both smaller fragments with low aspect ratio, extremely long and entangled nanofibers, and microfibers and bundles [19]. Thus, the three materials represented distinctively different nanocelluloses. CNC had a low aspect ratio compared to NFC and MFC. On the other hand, the structural content of MFC was highly heterogeneous compared to that of NFC and CNC. See Table 1 for summary of the structural properties of CNC, NFC and MFC.

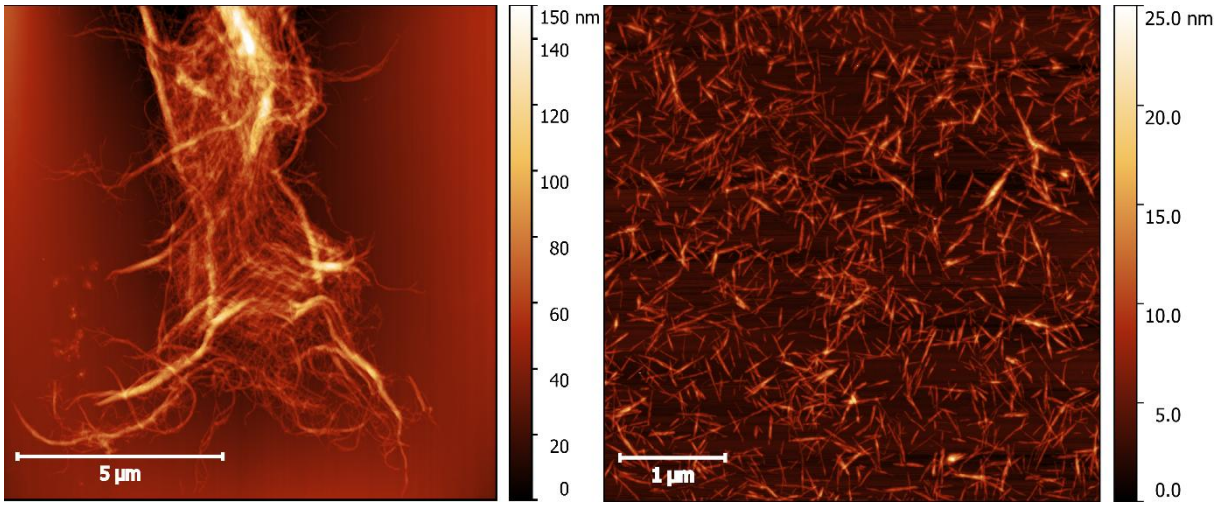

Figure 1. Atomic force microscopy (AFM) image recorded in tapping mode of NFC (left) and CNC (right) on a glass plate coated with polyethylenimine at 23°C and 48% relative humidity.

3.2. Characterization of the composite films

3.2.1. Swelling behavior

In previous work it was reported that the swelling of MFC-HPMC composite films increased with HPMC content and that a fraction of the of the HPMC was released from the films [7]. In this study, the swelling behavior of CNC-HPMC and NFC-HPMC films was investigated in Milli-Q water at 37°C for 100 and 180 minutes, respectively (Fig. 2a-b) and the results were compared with those previously reported for MFC-HPMC films (Fig. 3). Due to the fragile nature of CNC-HPMC composites, a modified method involving placement of the films in

baskets was used for submerging the films in the present work, see Materials and Methods. Even under these protective conditions the CNC-HPMC films with ≥ 20% HPMC rapidly lost mass and were fragmented, only maintaining coherency for about 100 minutes. CNC films containing less than 20% HPMC (w/w) remained coherent for the 180 minutes of the experiment (pure CNC films actually maintained structural integrity for more than one week). The swelling of NFC-HPMC films was possible to measure for 180 minutes.

The swelling of the NFC-HPMC films over time is presented in Fig. 2a. The films turned from opaque to white when exposed to the Milli-Q water. Regardless of HMPC content, the samples presented rapid initial swelling so that a plateau was reached already at the first time-point of 10 minutes. The largest swelling ratio of 11 g/g was obtained for the film with 35% (w/w) HPMC content. Generally, the swelling increased with increasing HPMC content, but the swelling's dependence on HPMC content may be non-trivial over time. A detailed analysis was not possible given the magnitude of the error bars.

The CNC-HPMC films presented a different trend in swelling with HPMC content (Fig. 2b) than the NFC-HPMC films. First, not all films reached a plateau within the 100 minutes of the experiment. It was noted that films with high HPMC content lost material over the experiment, as substantiated by the sample with 35% HPMC decreasing in weight between the last time points. Secondly, the CNC-HPMC films exhibited swelling ratios about ten times larger than the NFC-based films. Pure CNC films presented rapid initial swelling and reached a plateau at 6 g/g after 10 minutes, the value was slightly larger than for pure NFC films, but the behavior was qualitatively similar. The film containing 10% HPMC had larger swelling than the pure CNC film and did not reach plateau. At the same time the swelling ratio was lower for this film compared to CNC-based films containing more HPMC. The highest swelling ratio of around 75 g/g was obtained for the film containing 20% HPMC after 100 minutes, at which time the swelling was still increasing. The films containing 27% and 35% HPMC presented similar swelling behavior to the one with 20% HPMC up to 30 minutes. After this time the 20% HPMC film continued to swell, while the latter 27 and 35% HPMC films seems to reach a plateau at about 40 g/g. This was likely due to the swelling being counteracted by material being eroded from the films. To summarize, for CNC-HPMC films the swelling was larger and seemed to have a more complicated dependence on the HPMC content than for NFC-HPMC films.

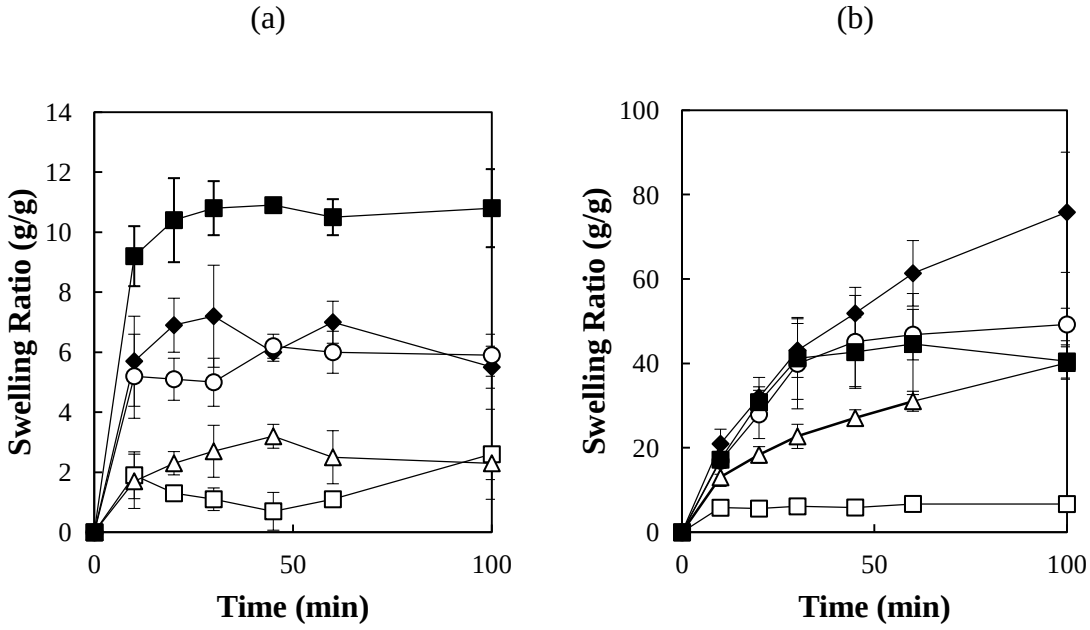

Figure 2. Swelling ratio versus time for (a) NFC and (b) CNC films with 0% (□), 10% (Δ), 20% (♦), 27% (○) and 35% (■) w/w HPMC. Error bars indicate standard deviation (n = 3).

In Fig. 3 comparison is made between the swelling ratios of CNC- (white), NFC- (grey) and MFC-based (black) films with varying HPMC content. The swelling ratios are reported up to 100 minutes. It can be seen that the swelling ratio is highest for CNC-HPMC films for all amounts of added HPMC.

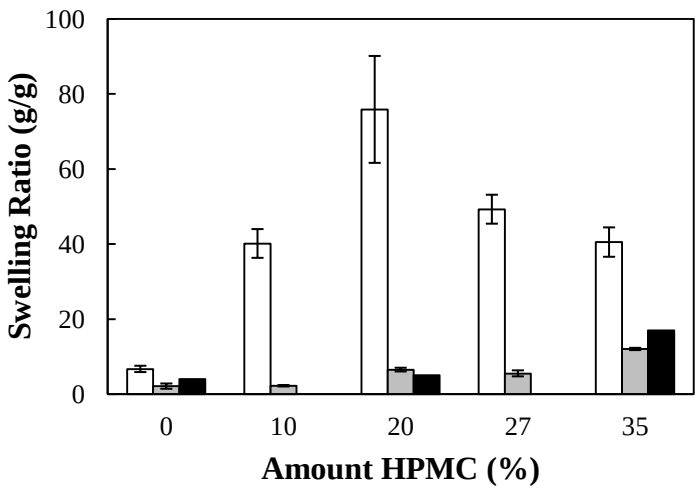

Figure 3. Swelling ratio for CNC-HPMC (white) after 100 minutes, NFC-HPMC (grey) and MFC-HPMC films (black) after 180 min. Error bars indicate standard deviation for CNC and NFC (n = 3). Data for MFC-HPMC are from [7].

For pure nanocellulose films the swelling ratio, measured as relative increase of mass, depends on the water ingress and displacement in the system. The water in swollen films of pure nanocellulose can be considered in two ways: (i) water is adsorbed to the surface of the nanocelluloses and to some extent penetrate into the nanocellulose fibers (leading to swelling of the nanofiber itself) and/or (ii) the pores are partly filled with water through capillary transport. The water transport can deform the film and lead to an increase of the macroscopic dimensions and a corresponding substantial decrease of the nanocellulose concentration. It is impossible to completely distinguish between these scenarios. However, if the main contribution to the swelling was water uptake of the fibers, a smaller swelling ratio would be expected for the crystalline CNC film compared to the two fibrous nanocelluloses. Since the opposite was observed (see Fig 3), it seems likely that the dominating mechanism for water uptake was capillary transport of water into the inter-cellulose space in the films.

The high swelling ratio of 75 g/g for 20% (w/w) CNC-HPMC composites and the swelling of the composite films in general can be rationalized by looking at the mechanism behind swelling of materials from water-soluble polymers. The first important step in this discussion is the mechanistic understanding of swelling of pure HPMC films, which coincides with the mechanism described in the literature for swelling of HPMC matrixes in controlled drug applications [25, 26]. When a dry HPMC material is exposed to water it will diffuse into the material, resulting in a water-concentration gradient. The water will plasticize the glassy HPMC, causing a transition to the rubbery state, in which the swollen material is best described as a semi-dilute polymer solution [27]. The rate of the water ingress into the material is determined in-part by water´s chemical potential gradient. One major factor that drives water diffusion and facilitates the dilution of the system (here seen as swelling) is the gain in conformation entropy of the HPMC chains. The dilution lead to a decrease in the polymer concentrations and when the HPMC concentration is close to or below the overlap concentration, the polymer will be disentangled and released from the surface of the film [28].

An interesting observation is that the swelling ratio versus time reaches a plateau for several of the HPMC/nanocellulose films (see Figs. 2a-b). To give a plausible explanation for this one need to discuss the factors counteracting the swelling process. These films contain a highly percolated fiber network that will prevent welling when the energy gain from further water absorption is balanced by the energy cost to deform the film. The shear modulus is higher for a network of longer fibers compared to that of a corresponding network of shorter fibers [29]. As such the energy cost of deformation should increase with fiber length. Therefore, for the

same amount of HPMC, i.e. the main driving force to swell the network, films of long fibers should present a lower equilibrium swelling than films of short fibers. This explains why films based on short CNC fibers swelled more than films based on longer NFC and MFC fibers for the same HPMC content (Fig 3).

The swelling ratio of a pure HPMC matrix tablet is known to be around 2, i.e. much less than what we observed for HPMC:nanocellulose films. A tentative explanation is that the highly percolated nature of the nanocellulose in the films provided a resistant armature that maintained film integrity and allow further swelling well beyond the point at which HPMC dissolve when used in a pure form.

In conclusion, we suggest that the driving force for swelling of HPMC-nanocellulose films is the presence of HPMC and that the counteracting force is the percolated network of nanocellulose, with longer NFC and MFC fibers restricting swelling more than shorter CNC fibers.

3.2.2. Loss of mass from films during swelling

The mass loss was determined at the final time point of the experiment and is presented in Fig. 4. The mass loss of NFC-based films appeared to have a linear dependence on HPMC content. Compared to the films based on MFC the loss of mass was less for all HPMC contents. This could be explained by that the heterogeneous MFC contained significant amounts of small-sized particles and aggregates of low aspect ratios [7]. Those aggregates might not have been effectively entangled in the MFC network and could thus leave the films. Interestingly, for both NFC and MFC the mass loss was less than the mass content of highly soluble HPMC. For CNC-based films the mass loss was similar as for NFC at HPMC contents of 0 and 10% (w/w). However, above 10% (w/w) HPMC there was a dramatic increase in mass loss for the CNC-based films and the mass loss was larger than the mass corresponding to HPMC content, meaning that a fraction of the CNC was lost as well. This dramatic increase in mass loss above 10% (w/w) HPMC content is in agreement with the mechanism for release of materials from hydrophilic matrix systems [28]. As mentioned above, the release of HPMC from pure HPMC matrix occurs when the dilution of the polymer reaches the regime of the so-called overlap concentration, where individual chains begin to be released. In a refined model accounting for shear forces around the matrix, the overlap concentration is replaced by

a critical polymer concentration at the outermost layer of the hydrophilic matrix. At the critical concentration the semi-dilute polymer solution cannot withstand the shearing forces caused by the stirring and therefore the polymer chains are released in the surrounding media. A similar mechanism can be applied to the HPMC-nanocellulose films. The nanocellulose network can withstand the shear forces above its percolation threshold. With an increased swelling the fiber concentration decreases and at high degrees of swelling the fibers can be eroded.

For the composite structures of HPMC and NFC or MFC, the ingress of water in the fiber network leads to dilution of the fiber network and HPMC. At low swelling ratios the strong armature nanocellulose fiber network can withstand the shear forces. However, hydrated HPMC will be diluted to concentrations around or below the overlap concentration and so that thus HPMC can disentangle and diffuse out from the films.

In the case of CNC-HPMC films the counteracting forces from the cellulose network on the swelling are low. For films with 10% (w/w) initial HPMC content a swelling ratio of 40 g/g and loss of mass of 7.4% was recorded after 100 minutes. The combined concentration of HPMC and CNC can be calculated to 2.2% (w/w) in this state (assuming a density equal to one). This is in the range of the percolation threshold of CNC [30, 31]. It is therefore likely that most of the HPMC had diffused out from the films but that the CNC network withstood the shear forces. Films with 20% (w/w) initial HPMC content presented a swelling ratio of 75 g/g and a mass loss of 60%. The combined concentration of HPMC and CNC can be calculated to 0.5% (w/w). This concentrations is below the percolation threshold of CNC and is in the range or below the overlap concentration of the HPMC used in this study [25]. Thus the mass loss was attributed both to dissolution of HPMC and erosion of the weak CNC network.

In conclusion, the loss of mass for both CNC- and NFC-HPMC composite films is suggested to be mainly due to dissolution of HPMC. However, for CNC-HPMC films with HPMC content above 10% the high swelling ratio and corresponding decrease in CNC concentration led to both HPMC and CNC being released from the films. This mechanism explain the swelling behavior of CNC-HPMC films and why the swelling of the 35 % (w/w) CNC-HPMC film seemingly passed through a maximum gravimetric swelling ratio over time. The same phenomenon is observed for hydrophilic matrix tablets [32, 33].

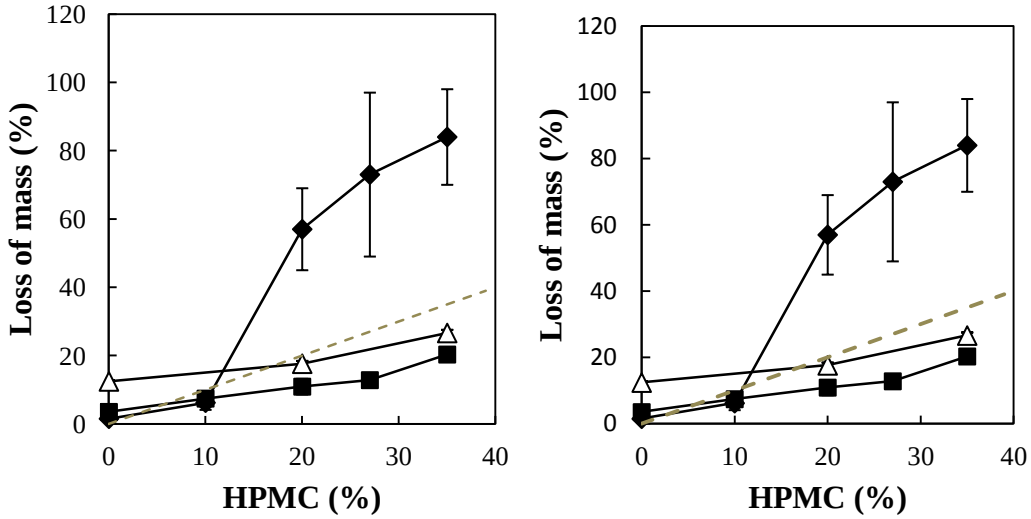

Figure 4. Loss of mass after swelling for CNC-HPMC (♦) (swollen for 100 min) and NFC-HPMC (■) and MFC-HPMC (△) (swollen for 180 min) films. Error bars indicate standard deviation (n = 3).The dashed grey line represent the maximal theoretical loss of HPMC.

3.2.3. Film morphology

The surface and cross-section morphology of the films prior to and after exposure to water was investigated with SEM. The surface of the films was homogeneous and did not show any distinct features. Fig. 5 shows the cross section of the CNC (a and c) and NFC (b and d) films containing 20% (w/w) HPMC. Fig 5a-b are images of the cross-section of dry films cleaved before exposure to water and Fig. 5c-d are the cross-section of the corresponding films after exposure to water for 30 minutes, followed by quenching in liquid nitrogen, cleavage and freeze-drying.

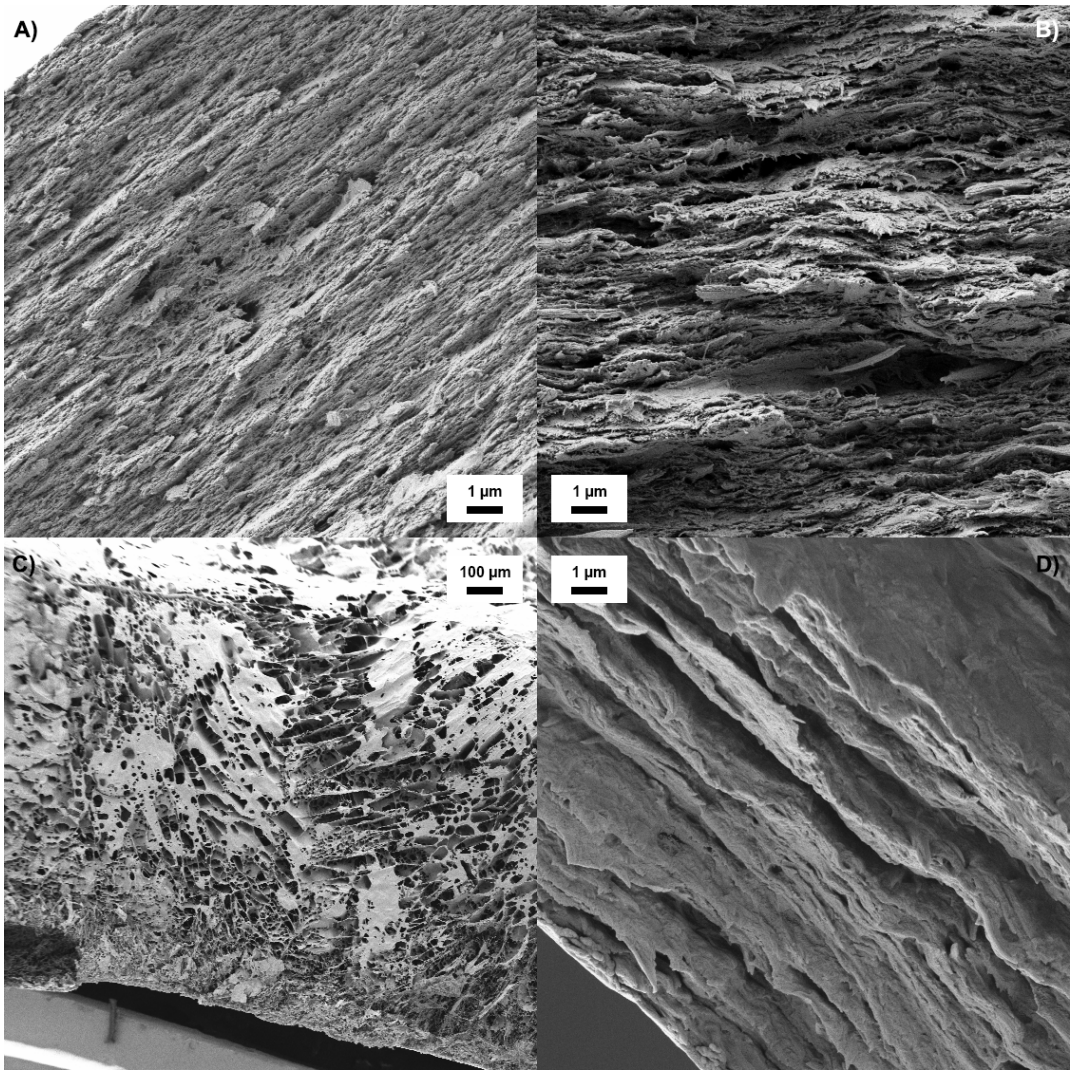

Figure 5. SEM Micrograph of a NFC and CNC films composed of 20% HPMC (w/w). (a) and (c) show the cross-section of CNC films after preparation before and after exposure to water, repesctively. Specimen (b) and (d) show the cross-section of the NFC films treated in the same way. The films exposed to water (c and d) were frozen in liquid nitrogen, cleaved and then freeze-dried. Note the 100 times larger scale bar in (c) compared to the other films.

The cross-section of the films after preparation showed that the CNC-based film was smother compared to the more fragmented/layered character of NFC based film, where each layer was estimated to be between 100 to 250 nm (Fig. 5). After exposure to water a highly swollen foam-like porous structure with large pores above 20 µm randomly oriented was observed for the CNC film, whereas the NFC films seemed to keep their layered structure aligned with the surface, in line with previous report for MFC [7]. Further interpretation on the pore-structure is rendered difficult as liquid nitrogen treatment is known to generate artifacts.

It seemed that the presence of HPMC did not significantly change the nanocellulose film forming properties, with CNC being more homogeneous while NFC formed a layered structure as previously observed [34, 35].

3.2.4. Mass transport properties

Having established differences in swelling behavior and film structure between CNC-based and NFC-based films and the similarity of the latter with MFC-based films, the wet-state barrier properties of the films were investigated. Tritiated water was used to monitor the water transport through the films at 37°C with stirring in both donor and acceptor compartments.

Pure films of CNC were too fragile to be placed in the diffusion cells, while pure NFC films as well as the composites could be analyzed. The corresponding data for the MFC-HPMC films was interpolated from previous work to simplify comparison [7]. The time dependency of the normalized radioactivity, *NRA*, of the tritiated water accumulated in the acceptor was plotted for CNC-, NFC- and MFC-HPMC films with various HPMC contents, as shown Fig. 6.

As expected from the similarities in swelling behavior and structure, the NFC-HPMC and MFC-HPMC presented similar mass transport properties. In addition, for both systems the transport across the films was decreased with increasing HPMC content. For the CNC-based films, the water transport through the films was slower than for NFC and MFC. As mentioned earlier, the CNC-films became very fragile and only the preparation with 10% (w/w) HPMC remained intact during the 180 minutes of the experiment. The transport of the tritiated water through the CNC-based films was similar irrespective of the HPMC content except for the higher fraction of HPMC (35% (w/w)) which showed lower mass transport rate. The trend in the transport through the nanocellulose films with different HPMC content can be more clearly seen by looking at the fraction of tritiated water in the acceptor compartment at a fixed time of 60 minutes (Fig. 7).

(a) (b) (c)

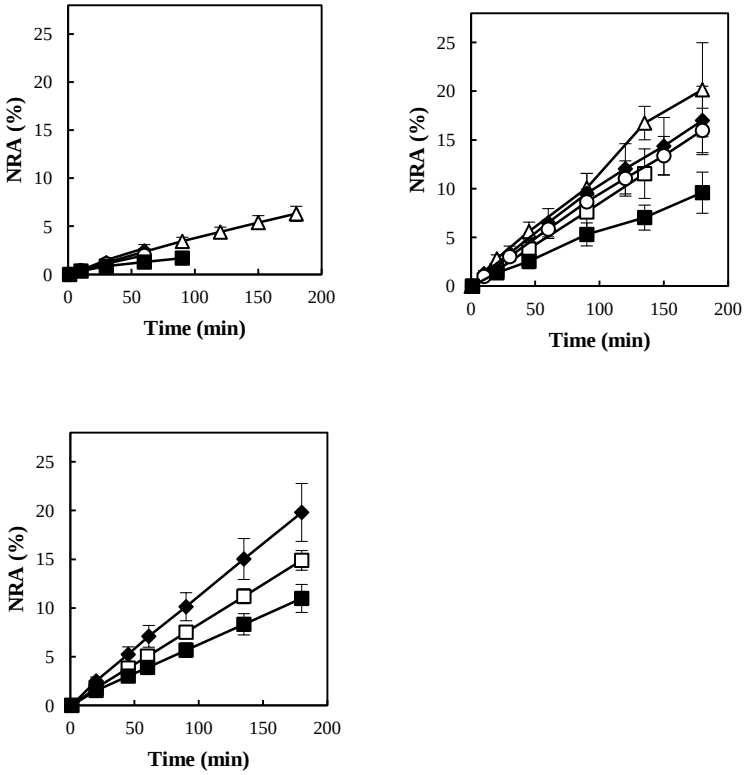

Figure 6. Normalized radioactivity in the acceptor after transport of tritiated water through films containing 0% (□), 10% (△), 20% (◆), 27% (○) and 35% (■) (w/w) HPMC. Error bars indicate standard deviation (n = 3). (a) CNC-HPMC; (b) NFC-HPMC; and (c) MFC-HPMC (n = 2 or 3). The same y-scale was used for all plots for a better comparison of the systems.

The mass transport rate across films depends on several of factors such as the level of hindrance the penetrant meets during the transport, typically fibers or polymer chains, the pathway for transport or the porosity of the system, for example. The CNC films will be more diluted (due to larger swelling and larger loss of mass) and thus have higher porosity than the NFC films. These properties should give larger mass transport for the CNC films compared to the NFC films. At the same time, an increased swelling of the films usually reduces the mass transport rate across the films due to an increased diffusion path. Fig. 7 shows that transport across CNC films was lower for all HPMC contents compared to the NFC and MFC films. This means that the reduction in mass transport due to the large swelling is dominating over the pore formation and dilution of the nanocellulose films.

In summary, pure NFC films and HPMC containing composites presented wet-state barrier properties almost identical to those of MFC-based films, despite differences in structural content of the two nanofibril celluloses and between film preparation methods. The results indicate that the barrier properties are robust with regard to film preparation and structural content of the used nanofibril cellulose. In contrast, the CNC-based films did display a lower permeability, but the films were highly unstable and their use as a wet-state barrier seems limited. Potential solutions to this problem could be to increase the stability of the films by incorporating a swellable polymer that forms a crosslinked network *in situ*.

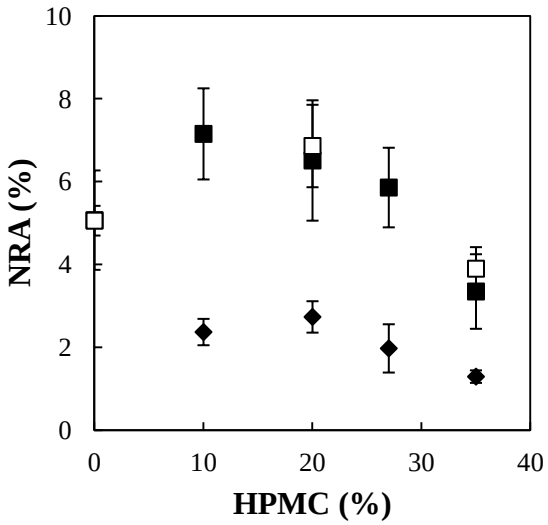

Figure 7. Normalized radioactivity in the acceptor after transport of water through films composed of CNC-HPMC (◆) NFC-HPMC (■) and MFC-HPMC (□) films after 60 minutes.

Conclusion

In this study, we investigated film properties for mixtures of the pharmaceutical approved cellulosic derivative HPMC with three different types of nanocelluloses. The length of the nanocelluloses in the HPMC:nanocellulose composite films appeared essential as it: (i) determined the structure of the formed composites: (ii) greatly impacted the films properties (swelling, mass transport, mass loss and integrity). Furthermore, a mechanistic model explaining the observed dependence on the fiber length was suggested. Briefly, long fibers in the network generate larger resistance to deformation than short fibers, resulting in larger swelling for networks of short fibers (like CNC). The main driving force for swelling in these

composites was the presence of the hydrophilic polymer (HPMC), which swelled and partly dissolved in water. The fiber network acted as an armature, which allowed a very large swelling of 75 g/g for the 20% (w/w) CNC-HPMC film after 100 minutes. At the same time, the mass loss of this film was as high as 60%, resulting in mechanical instability. For practical applications stable films are required and it is therefore important to tune the swelling by carefully choosing the length of used nanocellulose. For example, films from longer NFC fibers, also with 20% (w/w) HPMC, presented more restricted swelling (7 g/g) and were stable in water for more than a week. The increased diffusion length across the films due to swelling was the dominating factor in determining the water transport across the nanocellulose composite films. Even though the CNC-HPMC films were less dense and had larger mass loss, the water transport across them was slower than across corresponding NFC-HPMC films. Finally, all film properties were similar for films based on MFC or NFC, even though the films were prepared using very different methods. The NFC-HPMC films were sprayed using a spray gun, followed by drying at 50°C for several hours. MFC-HPMC films were produced by solvent casting for three weeks at under controlled conditions at 30°C. This indicates that the choice of manufacturing method for the films has much less influence on the film properties than the aspect ratio of the nanocellulose. The findings are highly relevant for further developments towards use of nanocellulose in wet-state applications

Acknowledgment

This project is part of the VINNOVA VINN Excellence Centre SuMo Biomaterials (Supermolecular Biomaterials—Structure dynamics and properties). The financial support from the Centre is gratefully acknowledged. Innventia AB is acknowledged for the kind gift of NFC.

References

[1] V. Kumar, R. Bollström, A. Yang, Q. Chen, G. Chen, P. Salminen, D. Bousfield, M. Toivakka, Comparison of nano- and microfibrillated cellulose films, Cellulose 21(5) (2014) 3443-3456.

[2] K. Syverud, P. Stenius, Strength and barrier properties of MFC films, Cellulose 16(1) (2009) 75-85.

[3] D. Klemm, F. Kramer, S. Moritz, T. Lindström, M. Ankerfors, D. Gray, A. Dorris, Nanocelluloses: A New Family of Nature-Based Materials, Angew. Chem. Int. Ed. 50(24) (2011) 5438-5466.

[4] N. Lavoine, I. Desloges, A. Dufresne, J. Bras, Microfibrillated cellulose – Its barrier properties and applications in cellulosic materials: A review, Carbohydr. Polym. 90(2) (2012) 735-764.
[5] S. Gardebjer, M. Andersson, J. Engstrom, P. Restorp, M. Persson, A. Larsson, Using Hansen solubility parameters to predict the dispersion of nano-particles in polymeric films, Polymer Chemistry 7(9) (2016) 1756-1764.
[6] S. Gårdebjer, A. Bergstrand, A. Larsson, A mechanistic approach to explain the relation between increased dispersion of surface modified cellulose nanocrystals and final porosity in biodegradable films, European Polymer Journal 57 (2014) 160-168.
[7] M. Larsson, J. Hjärtstam, A. Larsson, Novel nanostructured microfibrillated cellulose–hydroxypropyl methylcellulose films with large one-dimensional swelling and tunable permeability, Carbohydr. Polym. 88(2) (2012) 763-771.
[8] A.M. Slavutsky, M.A. Bertuzzi, Water barrier properties of starch films reinforced with cellulose nanocrystals obtained from sugarcane bagasse, Carbohydrate Polymers 110 (2014) 53-61.
[9] G. Rodionova, M. Lenes, Ø. Eriksen, Ø. Gregersen, Surface chemical modification of microfibrillated cellulose: improvement of barrier properties for packaging applications, Cellulose 18(1) (2011) 127-134.
[10] H.P.S. Abdul Khalil, Y. Davoudpour, M. NazrulIslam, A. Mustapha, K. Sudesh, R. Dungani, M. Jawaid, Production and modification of nanofibrillated cellulose using various mechanical processes: A review, Carbohydrate Polymers 99 (2014) 649-665.
[11] M. Samir, F. Alloin, A. Dufresne, Review of Recent Research into Cellulosic Whiskers, Their Properties and Their Application in Nanocomposite Field, Biomacromolecules 6 (2005) 612-626.
[12] M. Larsson, Q. Zhou, A. Larsson, Different types of microfibrillated cellulose as filler materials in polysodium acrylate superabsorbents, Chinese Journal of Polymer Science 29 (2011) 407-413.
[13] N. Lavoine, I. Desloges, C. Sillard, J. Bras, Controlled release and long-term antibacterial activity of chlorhexidine digluconate through the nanoporous network of microfibrillated cellulose, Cellulose (2014) 1-14.
[14] N. Lavoine, I. Desloges, J. Bras, Microfibrillated cellulose coatings as new release systems for active packaging, Carbohydrate Polymers 103 (2014) 528-537.
[15] R. Maren, D. Shuping, H. Anjali, L. Yong Woo, Cellulose Nanocrystals for Drug Delivery, in: K.J. Edgar, T. Heinze, C.M. Buchanan (Eds.), Polysaccharide Materials: Performance by Design, American Chemical Society, e-book, 2009, pp. 81-91.
[16] J.K. Jackson, K. Letchford, B.Z. Wasserman, L. Ye, W.Y. Hamad, H.M. Burt, The use of nanocrystalline cellulose for the binding and controlled release of drugs, International Journal of Nanomedicine 6 (2011) 321-330.
[17] P. Sakellariou, R.C. Rowe, E.F.T. White, Polymer/polymer interaction in blends of ethyl cellulose with both cellulose derivatives and polyethylene glycol 6000, International Journal of Pharmaceutics 34(1–2) (1986) 93-103.
[18] R.J. Moon, A. Martini, J. Nairn, J. Simonsen, J. Youngblood, Cellulose nanomaterials review: structure, properties and nanocomposites, Chem. Soc. Rev. 40(7) (2011) 3941-3994.
[19] M. Larsson, M. Stading, A. Larsson, High Performance Polysodium Acrylate Superabsorbents Utilizing Microfibrillated Cellulose to Augment Gel Properties, Soft Materials 8(3) (2010) 207-225.
[20] M. Pääkkö, M. Ankerfors, H. Kosonen, A. Nykänen, S. Ahola, M. Österberg, J. Ruokolainen, J. Laine, P.T. Larsson, O. Ikkala, T. Lindström, Enzymatic Hydrolysis Combined with Mechanical Shearing and High-Pressure Homogenization for Nanoscale Cellulose Fibrils and Strong Gels, Biomacromolecules 8(6) (2007) 1934-1941.

[21] D. Bondeson, A. Mathew, K. Oksman, Optimization of the isolation of nanocrystals from microcrystalline cellulose by acid hydrolysis, Cellulose 13 (2006) 171-180.
[22] M. Hasani, E.D. Cranston, G. Westman, D.G. Gray, Cationic surface functionalization of cellulose nanocrystals, Soft Matter 4(11) (2008) 2238-2244.
[23] J. Hjärtstam, T. Hjertberg, Studies of the water permeability and mechanical properties of a film made of an Ethyl Cellulose–Ethanol–Water ternary mixture, Journal of Applied Polymer Science 74(8) (1999) 2056-2056.
[24] L. Pranger, R. Tannenbaum, Biobased nanocomposites prepared by in situ polymerization of furfuryl alcohol with cellulose whiskers or montmorillonite Clay, Macromolecules 41(22) (2008) 8682-8687.
[25] A. Viridén, B. Wittgren, A. Larsson, Investigation of critical polymer properties for polymer release and swelling of HPMC matrix tablets, European Journal of Pharmaceutical Sciences 36(2–3) (2009) 297-309.
[26] A.R. Rajabi-Siahboomi, R.W. Bowtell, P. Mansfield, A. Henderson, M.C. Davies, C.D. Melia, Structure and behaviour in hydrophilic matrix sustained release dosage forms: 2. NMR-imaging studies of dimensional changes in the gel layer and core of HPMC tablets undergoing hydration, J. Controlled Release 31(2) (1994) 121-128.
[27] A. Körner, L. Piculell, F. Iselau, B. Wittgren, A. Larsson, Influence of different polymer types on the overall release mechanism in hydrophilic matrix tablets, Molecules 14(8) (2009) 2699.
[28] A. Körner, A. Larsson, L. Piculell, B. Wittgren, Molecular information on the dissolution of polydisperse polymers: mixtures of long and short poly(ethylene oxide), The Journal of Physical Chemistry B 109(23) (2005) 11530-11537.
[29] C.P. Broedersz, M. Sheinman, F.C. MacKintosh, Filament-length-controlled elasticity in 3D fiber networks, Physical Review Letters 108(7) (2012) 078102.
[30] V. Favier, H. Chanzy, J.Y. Cavaille, Polymer Nanocomposites Reinforced by Cellulose Whiskers, Macromolecules 28(18) (1995) 6365-6367.
[31] F. Du, R.C. Scogna, W. Zhou, S. Brand, J.E. Fischer, K.I. Winey, Nanotube networks in polymer nanocomposites: rheology and electrical conductivity, Macromolecules 37(24) (2004) 9048-9055.
[32] S. Abrahmsén-Alami, A. Körner, I. Nilsson, A. Larsson, New release cell for NMR microimaging of tablets: Swelling and erosion of poly(ethylene oxide), Int. J. Pharm. 342(1–2) (2007) 105-114.
[33] A. Körner, A. Larsson, Å. Andersson, L. Piculell, Swelling and polymer erosion for poly(ethylene oxide) tablets of different molecular weights polydispersities, J. Pharm. Sci. 99(3) (2010) 1225-1238.
[34] M. Henriksson, L.A. Berglund, P. Isaksson, T. Lindström, T. Nishino, Cellulose Nanopaper Structures of High Toughness, Biomacromolecules 9(6) (2008) 1579-1585.
[35] J. Huang, H. Zhu, Y. Chen, C. Preston, K. Rohrbach, J. Cumings, L. Hu, Highly Transparent and Flexible Nanopaper Transistors, ACS Nano 7(3) (2013) 2106-2113.